Examining the Functional Consequences of the Flexibility of Aminoglycoside Phosphotransferase (3')-IIIa

A Thesis Presented for the

Master of Science

Degree

The University of Tennessee, Knoxville

Katelyn Dawn Rosendall

May 2014

This thesis is dedicated to my parents and family who have encouraged me to dream big and to work hard, and to my fiancé Michael who has seen me through all of the craziness that dreaming big and working hard can bring.

“Where ever you go, go with all your heart”

-unknown

ACKNOWLEDGMENTS

I would first like to express my gratitude to my advisor, Engin Serpersu, who has made my success at the University of Tennessee possible through his guidance and encouragement. I would also like to thank the members of the Serpersu lab, in particular, Ed Wright, Sherin Raval, Xiaomin Jing, and past member: Adrianne Norris. I appreciate the help, laughter and encouragement that each of you have provided over the past year. I would like to acknowledge all the people who reviewed my thesis, your help was invaluable. And last, but certainly not least, I would like to thank the other members of my committee, Liz Howell and Gladys Alexandre, for their helpful feedback and ideas as I have worked to complete this project.

ABSTRACT

The use of aminoglycoside antibiotics began in 1940 with the discovery of streptomycin. The overuse and misuse of antibiotics has resulted in prevalent cases of antibiotic resistance. The most common source of aminoglycoside resistance is the presence of enzymes that covalently modify the antibiotics at specific locations. One such enzyme, APH(3′)-IIIa [the aminoglycoside phosphotransferase three prime three a] conveys resistance by transferring the γ-phosphate [gamma phosphate] from ATP [adenosine triphosphate] onto the 3′ [three prime] carbon of the aminoglycoside antibiotic sugar ring. APH(3′)-IIIa has been shown to be flexible in solution and this flexibility is proposed to be responsible for its large substrate profile. Upon binding the aminoglycoside, APH(3′)-IIIa adopts a well-defined structure. All previous experiments were conducted *in vitro*. Here, various aspects associated with the flexibility of APH(3′)-IIIa are further examined *in vivo*. In-cell NMR [nuclear magnetic resonance] experiments are used to determine the protein dynamics of APH(3′)-IIIa in the crowded environment of the cell. Next, the flexibility of APH(3′)-IIIa is examined when binding more rigid aminoglycoside antibiotics: sisomicin and netilmicin *in vitro*.

Table of Contents

Chapter I: Introduction 1

A. Aminoglycoside Antibiotics 1

i. Aminoglycoside general use and chemical structure 1

ii. Mechanism by which aminoglycosides cause cell death 3

B. Aminoglycoside Modifying Enzymes 3

i. Nomenclature and modification sites 3

ii. Substrate (aminoglycoside) promiscuity 4

C. Introduction to APH(3′)-IIIa 5

iii. APH structure 5

i. ATP and Aminoglycoside binding sites 6

ii. Dynamic nature of APH in solution 9

iii. Kinetics and thermodynamics of ligand binding 10

Chapter II: In-cell Nuclear Magnetic Resonance 13

A. Background 13

i. In-cell nuclear magnetic resonance spectroscopy 13

ii. Structural dynamics of APH 14

iii. Aminoglycoside in-cell effects 15

B. Experimental Procedures 15

i. Chemicals 15

ii. Growth of ^{15}N labeled APH cells 15

iii. Cell assays 17

iv. Cell lysis 18

v. In-cell nuclear magnetic resonance 18

vi. Empty vector in-cell nuclear magnetic resonance 19

C. Results/discussion 19
i. Optimization and visualization of APH in the cell 19
ii. In-cell structural changes of APH 20
Chapter III: APH flexibility allows binding to structurally rigid aminoglycosides 27
A. Background 27
i. Introduction to acetyltransferases(3)-IIa and IIIb 27
ii. Binding of sisomicin to acetyltransferases(3)-IIa and IIIb 28
iii. Formation of differing ternary complexes dependent upon order of addition 29
B. Methods 31
i. Chemicals and Reagents 31
ii. Growth and purification of APH 31
iii. Steady-state kinetics 32
iv. Isothermal titration calorimetry 32
v. Differential scanning calorimetry 34
vi. Nuclear magnetic resonance 34
C. Results/Discussion 35
i. Kinetic interactions of APH with sisomicin 35
ii. Thermodynamic interactions of APH with sisomicin and netilmicin 35
iii. Thermodynamics of the ternary complex formation are not dependent upon the order of addition 38
iv. Differential scanning calorimetry of APH complexes 39
v. Nuclear magnetic resonance of APH-siso complex 39
Chapter IV: Conclusion and future studies 49
References 52
Vita. 57

List of Figures

Figure Page

1. Aminoglycoside structures 2
2. Structure of APH(3′)-IIIa 8
3. APH NMR spectra difference with the addition of tobramycin 12
4. HSQC NMR spectra of APH with BSA and neomycin 22
5. LIVE/DEAD cell assays 23
6. SDS-Page of cell lysate 24
7. HMQC NMR spectra of APH in-cell fractions 25
8. HMQC NMR spectra of empty vector in-cell fractions 26
9. HSQC NMR spectra of AAC-IIa with tobramycin or sisomicin 30
10. ITC thermogram and isotherm of binary APH-sisomicin complex 43
11. ITC thermogram and isotherm of binary APH-netilmicin complex 44
12. Intrinsic enthalpy plot 45
13. DSC trace of APH complexes 46
14. HSQC NMR spectra of APH-sisomicin complexes 47
15. Structural model of APH 48

List of Tables

Tables

1. Thermodynamic parameters of binary complexes 41
2. Thermodynamic parameters of ternary complexes 42

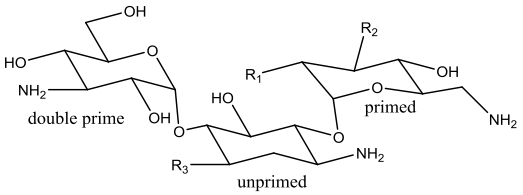
Chapter I: Introduction

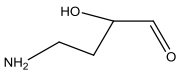
A. Aminoglycoside Antibiotics

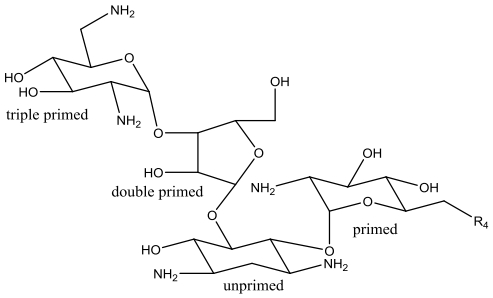
i. Aminoglycoside general use and chemical structure

Penicillin was the first antibiotic to be discovered and was used clinically in 1928. However, the term antibiotic was not used until 1941[3-5]. After the discovery of beta lactam antibiotics, aminoglycoside family antibiotics were the next to be discovered with streptomycin in 1940 [4]. Aminoglycosides can be used to treat both gram-positive and gram-negative bacterial infections. Aminoglycosides are known for treating tuberculosis as well as other serious infections; however, because of potent side effects their clinical use must be heavily monitored [6]. Currently, gentamicin, tobramycin, amikacin, streptomycin, neomycin, and paromomycin are approved by the US Food and Drug Administration for clinical use in the United States [7, 8]. Additional uses of aminoglycosides include the inhibition of HIV virus reproduction and treatment of some genetic diseases [9, 10] Streptomycin, like other aminoglycosides, is derived from soil bacteria and is synthesized from sugar monomers [11]. Aminoglycoside antibiotic structures contain a variety of sugar rings, with various modifications. The wide use of these antibiotics is possible in part because of variety in their chemical structures [4].

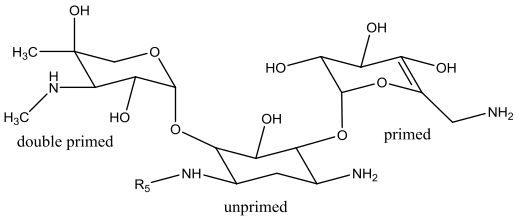
Most aminoglycosides are separated into one of two major groups, kanamycins and neomycins. The unprimed ring or aminocyclitol is the nucleus of both groups and is a 2-deoxystreptamine (2-DOS) ring linked by glycosidic bonds to other amino sugar rings (Figure 1) [12]. Aminoglycosides that are considered a neomycin contain a 4,5-disubstituted central 2-DOS ring, whereas those identified as a kanamycin contain a 4,6-disubstituted central 2-DOS ring [13]. There are numerous modifications that can be made to the various sugar rings to individualize the general backbone of the two groups of aminoglycosides, including but not limited to additional sugar rings, methyl groups, hydroxyl groups and amino groups (see Figure 1 for examples).



	R_1	R_2	R_3
kanamycin A	OH	OH	H
Kanamycin B	NH_2	OH	H
tobramycin	HN_2	H	H
Amikacin	OH	OH	



	R_4
neomycin B	NH_2
paromomycin	OH



	R_5
Gentamicin B	H
sisomicin	H
netilmicin	CH_3

Figure 1: Aminoglycoside antibiotic structures of kanamycin (top) and neomycin (middle) family representatives. Unprimed (2-DOS), primed and double primed rings are depicted. Gentamicin family representatives, gentamicin B, sisomicin and netilmicin are shown at the bottom. Gentamicin B is identical to sisomicin except that gentamicin B contains a saturated diamino primed ring, instead of an unsaturated diamino primed ring (shown).

ii. Mechanism by which aminoglycosides cause cell death

Aminoglycosides cause miscoding during protein synthesis which results in a compromised cell membrane and a reduction in cell viability [14]. First, aminoglycosides bind the aminoacyl-tRNA decoding site (A-site) on the 16S RNA subunit of the ribosome [15-17]. Crystal structure of the unbound 30S ribosomal subunit reveals that the A-site contains an internal loop in which two adenine side groups are facing into the helix. During translation, when the correct anticodon matches the codon of the mRNA, the two adenine side groups flip to face the outside of the helix. This conformational change dictates the continuation of translation [18]. The crystal structure of the 30S subunit bound by paromomycin reveals that the aminoglycoside inserts its primed ring into this helix, forcing the two adenines to pucker out from the helix [18]. The central unprimed ring of paromomycin interacts with several conserved base pairs in the A-site [15]. Therefore, the neamine portion (the prime and unprimed rings) of the aminoglycoside interferes with translation processes by binding structurally conserved regions of 16S ribosomal RNA (rRNA). This stabilizes a conformation of the A site which allows for incorrect ribosomal translation of proteins [16, 18]. The electrostatic forces between the positively charged aminoglycosides to the negatively charged RNA molecules drive this binding event [18]. Aminoglycosides have a ten-fold higher affinity to prokaryotic rRNA as compared to eukaryotic rRNA, providing a level of specificity for prokaryotic rRNA [15].

B. Aminoglycoside Modifying Enzymes

i. Nomenclature and modification sites

Antibiotic resistance is an increasing problem in clinical settings [19]. Resistance to aminoglycosides can occur via three main mechanisms: chemical modification of the aminoglycoside, chemical modification of the rRNA, and point mutations of the A-site [6, 18]. The main method of resistance is chemical modification of aminoglycosides by inactivating enzymes. The first enzyme, β-lactamase, found to provide resistance via chemical modification to β-lactam antibiotics was discovered in 1940 [20]. Today there are over fifty known enzymes that chemically modify aminoglycosides, termed aminoglycoside modifying enzymes (AGMEs) [19]. Each of these enzymes modifies the aminoglycoside at a

specific location, and is generally able to catalyze only one type of modification: phosphorylation, acetylation and adenylation. [19]. Therefore AGMEs are named according to site and type of modification made to the aminoglycoside. Enzymes that facilitate one of the listed modifications are termed phosphotransferases (APH), acetyltransferases (AAC), or nucleotidyltransferases (ANT) respectively. AGMEs are then further characterized by the location of the modification that they facilitate, for instance APH(3')IIIa phosphorylates the hydroxyl group attached to the C-3 on the primed ring of the aminoglycoside antibiotic [21]. Because there are several AGME's that catalyze the same modification, they are then further characterized by discovery and resistance profile [19].

Chemical modifications made to an aminoglycoside reduce its binding affinity for the A-site by creating steric hindrance or unfavorable electrostatic interactions with the 30S rRNA subunit. For instance, the addition of a negatively charged phosphate group alters the attraction of the aminoglycoside for the negatively charged A-site [15]. Chemical modifications at the various sites on aminoglycosides decrease their binding affinity for the A-site to varying degrees. The aminoglycoside side groups important to A-site binding are also important for recognition by AGMES. This makes designing drug targets exclusively for either the A-site or AGME difficult.

ii. Substrate (aminoglycoside) promiscuity

Aminoglycoside modifying enzymes are promiscuous. If the AGME is able to bind a large number of aminoglycoside substrates; thereby seeming to exhibit indiscriminant selectivity of substrates, it is termed highly promiscuous. For example, APH(3')-IIIa would be termed highly promiscuous because it is able to bind and modify to over a dozen aminoglycosides. AGMEs that are able to efficiently modify only a few aminoglycoside substrates are considered to have a low promiscuity. AAC(3)-IIa for instance is unable to provide resistance against neomycins, therefore AAC(3)-IIa has a lower promiscuity than APH(3')-IIIa. Other AGMEs, such as AAC(3)-IVa have even more restricted substrate promiscuities [19].

C. Introduction to APH(3′)-IIIa

As mentioned before, each AGME has a specific binding profile as well as binding mechanism. This thesis will focus on AGME APH(3′)-IIIa which will be referred to as APH. The structure and mechanism of APH will be described here; however additional AGMEs with differing structures and mechanisms will be discussed in lesser detail in chapters III and IV.

APH is a 31 kDa protein produced by gram-positive *cocci* such as *Staphylococci* and *Enterococci.* Functionally, APH catalyzes an adenosine triphosphate (ATP) dependent phosphorylation of hydroxyl groups at the 3′ position of aminoglycosides [1]. APH is known to modify aminoglycosides: kanamycin A, kanamycin B, neomycin, paromomycin, ribostamycin, lividomycin (modifies the 5″ hydroxyl), butirosin, gentamicin B, amikacin, and isepamicin, but binds additional aminoglycosides that do not contain a 3′ hydroxyl group such as tobramycin [19, 22].

iii. APH structure

APH is found as either a monomer or a covalent dimer, linked by two disulfide bridges: Cys19 is linked to Cys156 of the partner molecule and vice versa [1]. Crystal structure of APH solved by Hon *et al.* shows APH as a dimer, with each monomer bound to an ADP molecule as well as two magnesium ions (Mg^{2+}) and several solvent molecules. The monomers are linked in a head-to-tail-tail-to-head orientation [1]. The two active sites face each other and are separated by approximately 20 Å [1]. However, in physiological conditions APH is most likely to be found as a monomer [23]. In experiments described here, purified APH is kept in a monomeric state by incubation with dithiothreitol (DTT), a redox reagent that reduces disulfide bonds of exposed cysteine residues. APH is then stored in a Tris(2-carboxyethyl)phosphine hydrochloride (TCEP-HCl) containing buffer which also reduces disulfide bonds but is considered more stable than DTT [24].

Although APH shares very little sequence homology with other protein kinases, it contains several structural features associated with protein kinases. APH is made up of two lobular regions: the N-terminal region and the C-terminal region [1]. The N-terminal region is made up of 94 residues and is the smaller lobe. The larger C-terminal lobe is made up of 157 residues. The lobes are connected by a stretch of twelve residues that form a short β

strand and an α helix [1]. The N-terminal lobe contains a five-stranded antiparallel β sheet (strands labeled β1-β5) with an α helix located between strands 3 and 4; following the β sheet is another short helix. The structure of the N-terminal lobe region as well as the linking region is consistent with other eukaryotic-type protein kinases. However, APH lacks the highly conserved G-X-G-X-X-G motif seen in typical protein kinases located in between beta strands β1 and β2 [1]. The C-terminal lobe region is subdivided into a central core region, insert region, and C-terminal region. The central core is made up of helices α4 and α5 with a hairpin-shaped loop that contains a short antiparallel β sheet. This region also shares conformational similarity with other protein kinases [1]. The insert region consists of two helices (αA and αB) connected by a 19-residue loop. The C-terminal region is made up of two helices (αC and αD). Both the insert region and the C-terminal region of the C-terminal lobe differ from the typical protein kinase C-terminal fold. A topological depiction of the APH structure is given in Figure 2.

The 60 residue insert region of APH is particularly interesting. Much smaller in most protein kinases, this region is responsible for specificity and selectivity of substrates. X-ray crystallography showed that the insert region is located in front of the active site, and is in a position to interact with aminoglycoside substrates of APH [1].

i. ATP and Aminoglycoside binding sites

Binding of substrates with APH follow Theorell-chance mechanism, meaning that there is an order to substrate binding. ATP and Mg^{2+} ions bind the enzyme first, followed by the aminoglycoside. After the phosphate transfer from ATP to the antibiotic, the phosphorylated aminoglycoside is released followed by the release of ADP [23, 25]. At typical intracellular ATP concentrations the ATP binding site of APH will be saturated [26]. All aminoglycoside phosphotransferase enzymes share a common active site motif. The ATP active site is found in the linking region between the N-terminal lobe and the C-terminal lobe. [23]. According to crystal structures, the adenine ring of ATP is buried, forming several interactions with both N-terminal lobe and C-terminal lobe residues. The α-phosphate interacts with two water molecules, highly conserved residue Lys44, as well as the first Mg^{2+}. The β-phosphate was found to interact with one water molecule, Lys44, Ser27 as well as the second Mg^{2+}. The donor phosphate or γ-phosphate coordinates with

both magnesium ions [23]. The two magnesium ions facilitate the correct orientation of the nucleotide when binding to APH.

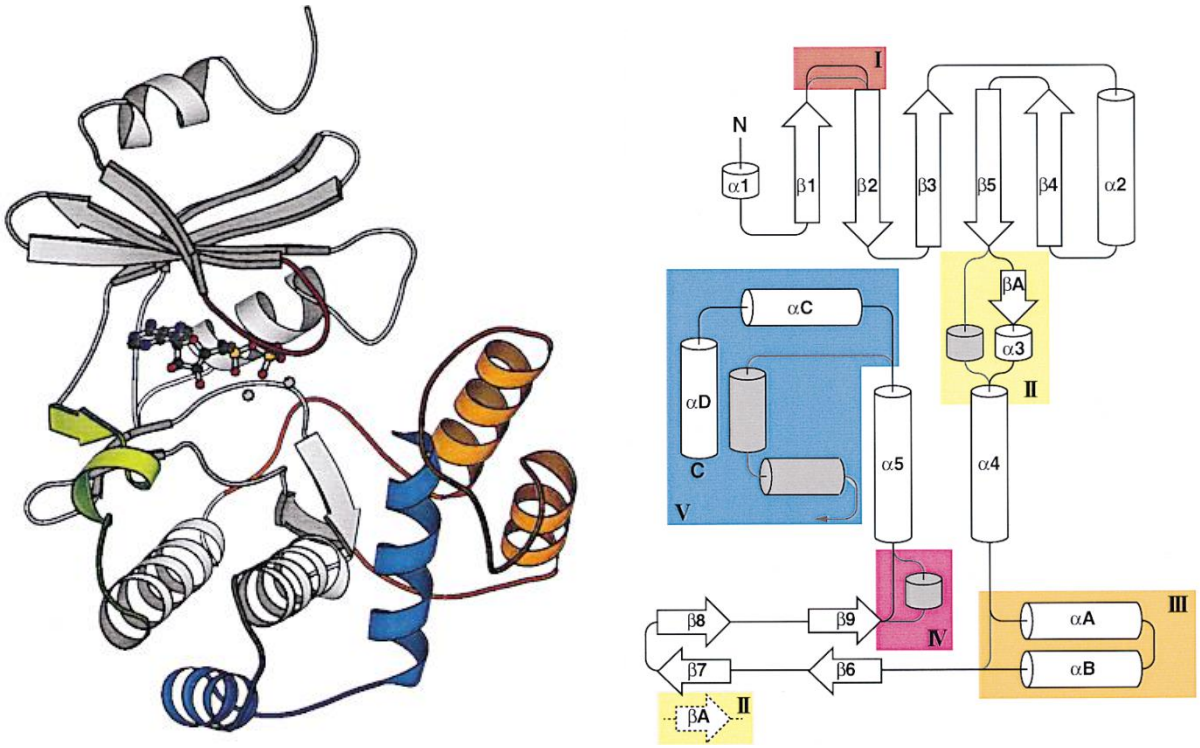


Figure 2: structure of APH, high lighting the GXGXXG region (red), flexible binding loop (orange), insert region (purple) and tethering segment (yellow). Topological diagram of the secondary structure highlights the same regions and provides a comparison to typical eukaryotic protein kinase secondary structure (shown in grey) [1].

Crystal structure analysis of apo APH compared to ADP bound APH revealed the interaction of a short loop region (residues 22-29), between β1 and β2, with the binding of the ATP molecule. These residues occupy part of the nucleotide binding region in the absence of nucleotide, but shift outward in the presence of nucleotide [23].
The same electrostatic forces that are important for the binding of the aminoglycoside to rRNA are also important in the binding of aminoglycosides to APH. The aminoglycoside binding pocket contains three aspartic acid residues, five glutamic acid residues and the C-terminal carboxylic acid group. The positively charged aminoglycosides are attracted to the excess negative charge of APH in the region of its binding site [15]. Crystal structures of APH bound with ADP and kanamycin A or neomycin B showed that the flexible loop region from 147-170 moves approximately 10 angstroms from unbound to bound state. It is thought that Glu157, Asn158, and Glu160 from this loop region interact with the aminoglycoside substrate [27]. It is predicted that similar to other protein kinases, an aspartate (Asp190) is responsible for the catalytic activity of deprotonating the substrate hydroxyl group. It has been suggested that there is a direct transfer of the phosphate group onto the aminoglycoside, however the exact mechanism by which APH phosphorylates its bound aminoglycoside substrate is still unknown [23].

ii. Dynamic nature of APH in solution

In previous work done by Norris *et al.* it was shown that in the absence of ligand, APH has a highly overlapped heteronuclear single quantum coherence (15N-1H HSQC- henceforth will be referred as HSQC) nuclear magnetic resonance (NMR) spectrum [28]. This overlapped spectrum indicates that several backbone amide groups are in very similar chemical environments, suggesting that the apo enzyme is flexible and may be adopting multiple confirmations in an aqueous solution. Hydrogen-deuterium exchange studies with APH revealed that after 15 minutes of exposure to deuterium oxide (D_2O), 80% of the backbone amides had fully exchanged and were 100% exchanged after 15-20 hours [28]. When APH is part of a binary complex with kanamycin A the $HSQC_{H2O}$ spectra is dramatically different as compared to the apo form. When bound to antibiotic, approximately 85% of all resonances were well-resolved [28, 29]. The chemical shifts seen with the binary APH-aminoglycoside complex indicated that APH adopts a more well-

defined structure when bound to aminoglycoside antibiotics (Figure 3) [28]. Hydrogen deuterium exchange experiments done with APH bound to either kanamycin A or neomycin B showed significant increase in the protection of backbone amide groups [28]. There were also differences in protection of specific amino acids between the bindings of kanamycin A or neomycin B. This indicated that the effect of ligand binding to APH resulted in different structural and dynamic properties dependent upon the ligand [28].

iii. Kinetics and thermodynamics of ligand binding

When discussing the complexes of APH, the term binary will refer to the complex of either antibiotic or adenylmethylenediphosphnate (AMPPCP) bound to AGME. AMPPCP is a non-hydrolysable analog of ATP. The term ternary will refer to the complexes formed with APH, aminoglycoside, Mg^{2+} and AMPPCP. In theory, this not a ternary complex because two Mg ions bind to APH therefore, equaling a total of five binding partners. For the purpose of this study Mg^{2+} was kept at saturating levels in both samples during titrations when AMPPCP was used. Therefore the only one component is binding to the formed complex of the other four. The order of addition is found in the ternary nomenclature, for example the formation of ternary complex APH-antibiotic-Mg-AMPPCP was created by adding Mg-AMPPCP into APH-antibiotic-Mg complex.

Binary thermodynamic studies done of APH binding to various aminoglycoside partners revealed that, in general, binding is enthalpically driven which is compensated for by an unfavorable entropic contribution [30, 31]. The overall gain in structure upon the binding of aminoglycoside to APH correlates well as a potential source for the unfavorable entropy (ΔS). Published negative enthalpy (ΔH) values associated with the formation of the binary complex indicate that formation is driven by favorable binding contacts such as polar, electrostatic, van der Waals forces and hydrogen bonds [30]. The large exothermic heat of association is able to compensate for the unfavorable entropy, therefore association of APH and all aminoglycosides have a favorable Gibb's energy change (ΔG). Isothermal titration calorimetry (ITC) of ternary enzyme-CaATP-aminoglycoside complexes revealed that when CaATP is present, binding of the aminoglycoside to APH is generally tighter [30]. As stated previously, APH exhibits a Theorell-Chance kinetic mechanism of binding; in this case the binding of CaATP seems to encourage binding of aminoglycoside.

APH is the most well-studied aminoglycoside modifying enzyme to date, however the exact mechanism by which it is able to modify such a large number of substrates remains to be fully elucidated [9]. Here we will further examine various aspects of the flexible nature of APH.

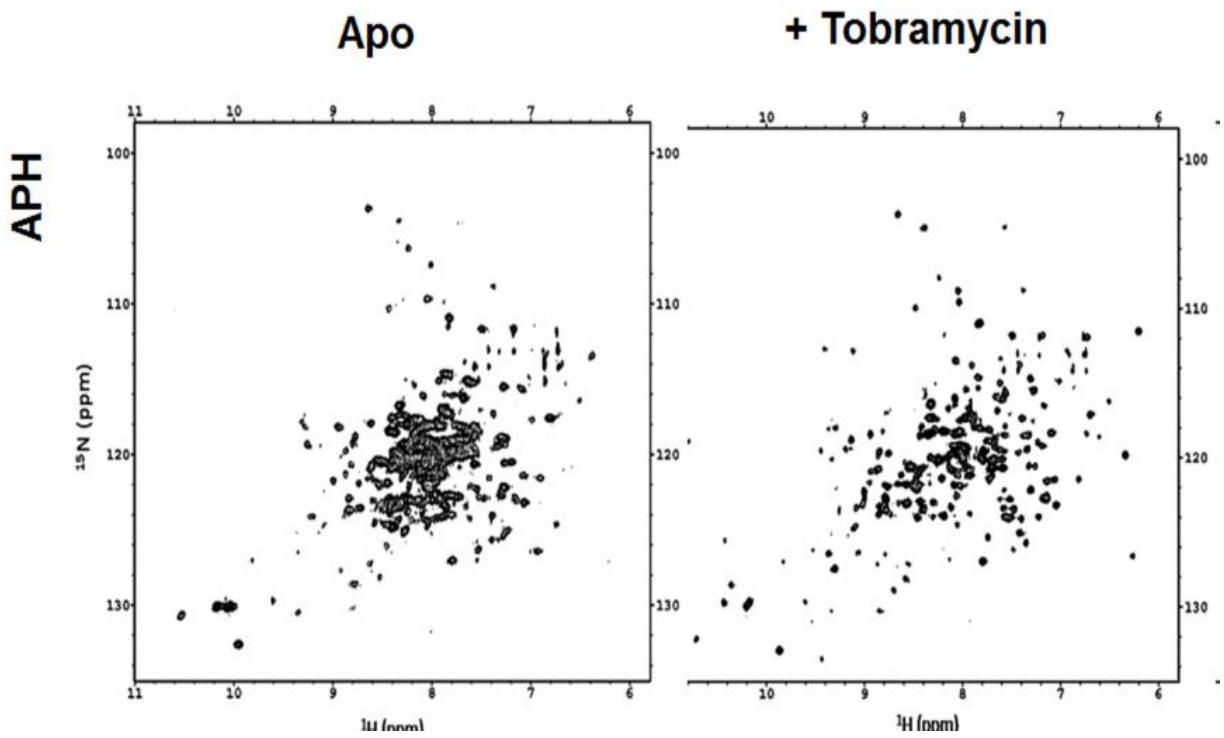


Figure 3: Partial image used with permission of Norris *et al.* HSQC NMR spectra of APH complexes. APH in its apo (left) and binary APH-tobramycin (right) forms are shown. All spectra were taken under similar experimental conditions and shown to matching contour levels [2].

Chapter II: In-cell Nuclear Magnetic Resonance

A. Background

i. In-cell nuclear magnetic resonance spectroscopy

The first NMR spectrometer became commercially available in 1961 with the 60 megahertz (MHz) Varian A-60 [32]. Typical NMR experiments involve the examination of small molecules and macromolecules *in vitro*, currently NMR techniques are also being used to determine the dynamics of proteins *in vivo*. Termed "in-cell" NMR spectroscopy, this technique is valuable as it uses NMR to investigate the conformation as well as the dynamics of proteins while they are in their native cellular environment. The cellular environment is crowded, with macromolecular concentrations as high as 400 g/l. Most proteins are studied outside the cell with concentrations of 10 g/l or less [33]. There can be discrepancies between protein dynamics studied *in vitro* by NMR and those that are studied in the more dilute *in vivo* environment. Therefore the use of in-cell NMR techniques provides a unique opportunity to examine the naturally found dynamics of a protein. However, it is unlikely that in-cell NMR spectroscopy will replace *in vitro* NMR experiments as the latter offers sharper line widths and more stable conditions for experiments over longer periods of time. In-cell NMR requires that the protein of interest be labeled, as well as contained in an intact live cell. Labeling is required to make the protein of interest distinguishable from the resonances of all other proteins in the cell. The most common forms of labeling are with ^{13}C, ^{15}N, and ^{19}F [34]. Labeling requires the use of expression vectors to overexpress the protein of interest in labeled media.

In more commonly used NMR experiments, proteins are able to tumble freely in solution and have rotational correlation times that are less than a few nanoseconds [34]. Increasing viscosity of a solution results in a slowed tumbling of the protein and in a broadening of the resonance lines. Proteins in the cell are subjected to environments of higher viscosity and therefore a broadening of resonance lines is to be expected. This broadening results in a loss of resonances of more structured portions of the protein. Larger line widths associated with in-cell NMR result in greater peak overlap relative to their *in vitro*

counterpart. Therefore it is important to only compare changes occurring in different in-cell experiments, rather than to *in vitro* experiments. In-cell protein leakage is a common problem associated with in-cell NMR. As the cells are stressed they experience cell damage and the labeled protein is released (protein leakage). It was previously reported that leaked proteins will cause artifacts, therefore careful measures must be taken to ensure that the cells are healthy [33]. Heteronuclear multiple-quantum coherence (HMQC) experiments are used with in-cell experiments for their quickness of completion with relatively little loss in peak resonance.

ii. Structural dynamics of APH

Previous H/D exchange NMR experiments showed that the APH backbone amides exchange rapidly, confirming that APH is flexible in solution [28]. This flexibility is hypothesized to allow APH to be highly promiscuous. In 2010 the backbone resonance assignments were made for the APH-tobramycin complex [29]. This work confirmed and expanded on previous NMR work with APH; the 7.5-9 ppm peak range seen with the apo complex increases to 115-121 ppm range when bound to tobramycin making it possible to assign more of the resonances [28].

The crowded nature of the cell can be to an extent mimicked by the addition of crowding agents such as bovine serum albumin (BSA), glucose or albumin [34]. Preliminary data showed that with the addition of BSA, the HSQC NMR spectra remained fairly overlapped as compared to the HSQC NMR spectra of apo APH complex without BSA. This indicates that even in a crowded environment, ^{15}N labeled APH retains much of its flexibility, shown by the retention of highly overlapped spectra (Figure 4).

Neither crystallography nor typical NMR studies have looked at the enzyme's dynamics in its natural environment. New NMR techniques have provided a way to examine protein dynamics while still contained in the cell. Although this method is still being developed, it is useful when determining the effects of crowding on a protein's dynamics. Therefore, in-cell NMR techniques will be used to look at the structural dynamics of APH when overexpressed in *Escherichia coli* cells.

iii. Aminoglycoside in-cell effects

Aminoglycoside antibiotics enter both gram-positive and gram-negative bacteria via three distinct steps. First is the self-promoted uptake of the antibiotic by binding onto anionic compounds like phospholipids to promote an increase in uptake of the antibiotic into the periplasmic space [12, 35]. Next, the electron transport system creates a electrochemical gradient across the mitochondrial membrane, which facilitates the uptake of antibiotics into the cytoplasm by unidentified transporters [12]. The aminoglycoside antibiotics then cause errors in protein synthesis. The mistranslated membrane proteins then allow for increased uptake in antibiotics which further accelerates cell death [12, 14, 15, 18]. In order to see conformational changes associated with binding of APH to an aminoglycoside in the cell, the choice and amount of aminoglycoside will need to be optimized. The amount of aminoglycoside will need to be low enough to maintain cell viability and therefore cause low amounts of cell leakage, but high enough concentrations so that APH will be in its bound form.

B. Experimental Procedures

i. Chemicals

Isopropyl-β-D-thiogalactopyranoside (IPTG) was purchased from Inalco Spa (Milan, Italy), and 99.9% deuterium oxide was obtained from Cambridge Isotope laboratories (Andover, MA). ^{15}N enriched salts were also purchased from Cambridge Isotope Laboratories (Andover, MA). All other general chemicals and aminoglycosides were of highest available purity and were obtained from either Sigma-Aldrich (St. Louis, MO) or Fisher Scientific (Pittsburgh, PA).

ii. Growth of ^{15}N labeled APH cells

Following closely to methods previously used, agar plates (10 g/l tryptone, 5 g/l yeast extract, 10 g/l NaCl, 15 g/l agar) containing 100 μg/ml ampicillin (amp) and 50 μg/ml kanamycin A were streaked with transformed *E.coli* [33, 34]. The transformed cells contained a pET-15b vector with the genetic information to overexpress APH, generously provided by Dr. Amber Bible and Dr. Adrianne Norris. Ampicillin (AMP), while not an

aminoglycoside is used because this particular expression vector codes for ampicillin resistance via the expression of the enzyme β-lactamase. Resistance to ampicillin, as well as overexpression of APH which provides resistance to kanamycin A, ensured that the colonies grown contained the correctly cloned pET-15b vector [36]. An extra agar plate was created each time and contained both antibiotics, but was not streaked. This was done as a negative control. Plates were inverted and incubated overnight at 37 °C. The next afternoon, a single colony was inoculated into approximately 15 mls fresh Luria Broth (10 g/l tryptone, 5 g/l yeast extract, 10 g/l NaCl) containing 100 µg/ml AMP and incubated at 37 °C with agitation of 200 RPM overnight. The following morning the overnight culture was used to seed a fresh 100 ml Luria Broth (LB) and AMP culture. The fresh culture was then allowed to grow at 37 °C with agitation until it reached 0.4 OD_{600}. To ensure that the cells used for in-cell NMR were healthy, the cultures were kept at cell concentrations lower than 0.5 $OD_{600.}$ This ensured that the cells were actively growing and not in stationary or death phase when induced.

Cells were then transferred to 50 ml centrifuge tubes where they were spun at 1600 xg for 15 minutes. The Luria broth was then decanted and cells were suspended in 70 ml of ^{15}N labeled M9 media. Ingredients for 1 Liter final volume of M9 minimal media are as follows: 7 g/l sodium phosphate, 3.5 g/l monobasic potassium phosphate, .5 g/l NaCl, 1 ml trace metal solution, 1 ml 1M $MgSO_4$, 100 µl 1M $CaCl_2$, 70 µl .5M $FeCl_2$, 25 µl 2% thiamine, 4 g glucose, 1 g $^{15}NH_4Cl_2$, and 100 µg/ml AMP [28]. The M9 minimal media is filter sterilized and kept at 4 °C until use. The trace minerals solution was made with a final volume of 1 liter and contained 2.86 g H_3BO_3, 1.81 g $MnCl_2*7H_2O$, 0.23 g $ZnSO_4*7H_2O$, 0.39 g $Na_2MoO_4*2H_2O$, 0.079 g $CuSO_4*5H_2O$, and 0.0494 g $Co(NO_3)_2*6H_2O$, which was filter sterilized and kept at 4 °C. The culture was placed at 37 °C with agitation for 10 minutes before adding 700 µl of 0.024 g/ml IPTG. The time delay was to allow the cells to acclimate to the new media and restart growth. Cells were not initially grown in ^{15}N labeled media so that only the induced protein would be labeled. IPTG mimics allolactose in the cell; it binds onto the lac repressor which then allows for transcription of APH which is located in the lac operon. IPTG is not hydrolyzed by β-galactosidase and therefore remains at a constant concentration, encouraging consistent overexpression of APH. An induction time of 4 hours

was initially used to produce an increased expression of APH. High concentrations of APH are desirable, as it is difficult to get a good signal from the ^{15}N labeled protein in the crowded environment of the cell. However, because of the reduced cell viability at high induction times, the induction time was later reduced to 30 minutes. Cells were then transferred to clean 50 ml centrifuge tubes and spun at 1600 xg for 10 minutes, which produced a very fragile pellet of cells. The M9 media supernatant was decanted off and cells were then gently suspended in 1200 µl of 7-10% deuterated PBS buffer (3.2 mM Na_2HPO_4, 0.5 mM KH_2PO_4, 1.3 mM KCl, 135 mM NaCl with added 7-10% volume D_2O pH 7.4) by gentle swirling.

iii. Cell assays

To determine the best condition in which to perform in-cell NMR, LIVE/DEAD cell assays were used to analyze cell viability. Cells were grown under several different conditions and induction times, they were then stained according to the LIVE/DEAD BacLight Bacterial Viability Kit protocol[37]. Although the chemical structures of these stains are copy-righted, it is well documented that the SYTO 9 dye is a green fluorescent nucleic acid stain that labels the cell membrane. The red-fluorescent nucleic acid stain, propidium iodide, is able to penetrate cells with damaged cell membranes [37]. The emission wavelengths for the fluorescent stains are 500 nm for the SYTO 9, and 635 nm for propidium iodide. Cells that fluoresced at 500 nm were considered alive and cells that fluoresced at 635nm were considered dead. Using a Zeiss Observer .Z1 microscope, cells were visualized using oil emersion 63 x objective, which has a resolution of 0.24 micrometers. Cells were observed under differential interference contrast (DIC) filter as well as filters for green fluorescent protein (GFP) and red fluorescent protein (RFP). The GFP filter collects emission wavelengths at 510 nm and the RFP filter collects emission at 700 nm. Pictures were taken of each condition using a Hamamatsu ORCA-ER digital camera attached to the microscope, and saved in OpenLab5 software. All DIC, GFP and RFP images were taken sequentially after switching the excitation wavelength. Images were then analyzed via Image J software where live and dead cells were counted on each image [38]. The numbers of live or dead cells were analyzed and graphed using Graphpad Prism software.

iv. Cell lysis

Small sample size prevented use of the French press to lyse the cells [30]. Sonification was also not applicable as it was previously shown to deactivate APH. Therefore cell lysis trials were done using various combinations of freeze-thaw cycles and the addition of lysozyme. Preparation of cells began according to the method outlined in section *ii* above, with the following variations: unlabeled ammonium chloride was used during induction and cells were suspended into 10 mls of non-deuterated PBS buffer. The sample was then separated into ten 1ml aliquots. Each aliquot was subjected to a different combination of freeze thaw cycles by freezing in liquid nitrogen and thawing at room temperature and addition of lysozyme. Lysozyme was used because of its known ability to damage bacterial cell walls [39]. The protocol for using lysozyme in cell lysis calls for a heat shock of the sample in order help break apart the cell wall, however heat above 45 °C denatures purified APH protein therefore in order to have fully active enzyme heat shock was not used in the varying lysis conditions [40]. Among the conditions tried, several included adding lysozyme preheated as well as unheated. Each aliquot was then centrifuged at maximum speed for 2 minutes. 38 µl of supernatant from each sample was combined with 12 µl 4% SDS loading dye and loaded into a lane on a 10% acrylamide gel [41]. The gel ran at 85 volts for approximately 45 minutes. It was then stained it for 20 minutes, followed by destain for 1.5 hours. Methods followed and materials used were in accordance with previously published work [41, 42].

v. In-cell nuclear magnetic resonance

For in-cell NMR experiments, 1200 µl of prepared whole cell sample was transferred to a NMR tube. The whole cell sample was then inserted into the 600 MHz NMR spectrometer. After appropriate calibrations are performed, a 1 hour HMQC experiment with 32 scans was executed. Upon completion of the experiment, cells were transferred to a microcentrifuge tube and spun in a table top centrifuge at 2,000 RPM for 10 minutes. 600 µl of the supernatant was then transferred to a clean NMR tube and an identical HMQC experiment was run after re-calibrating the NMR machine. The supernatant is run separately because it must be shown that the protein has not leaked from the cell. If the protein has leaked into the extracellular space it is not subjected to the same crowding

effects as the in-cell protein. The pelleted cells are then lysed according to our determined protocol of alternative freeze-thaw cycles. The cell debris was then centrifuged for 10 minutes at 13.2 RPM. Upon cell lysis, the labeled APH protein is freed from the cell and located in the cell lysate. 600 µl of the cell lysate is transferred to a clean NMR tube and an identical HMQC experiment is performed. Spectra were processed in nmrDraw and exported to Sparky for analysis and display [43, 44]. Adobe Photoshop software was used to invert images to change the background to white.

vi. Empty vector in-cell nuclear magnetic resonance

An important negative control was in-cell NMR performed on cells containing an empty vector. This was done to determine the amount of ^{15}N that is nonspecifically incorporated into the cell. First, competent *E.coli* cells were transformed with an empty pET-15b vector. Proper transformation was confirmed by sequencing to ensure that the vector was empty. The empty vector strain of *E.coli* was then grown using the same procedures previously described in section ii. Identical in-cell HMQC NMR experiments were performed and analyzed.

C. Results/discussion

i. Optimization and visualization of APH in the cell

The first source of protocol optimization was to reduce the amount of protein leakage from the cell. LIVE/DEAD cell assays were performed on cells grown under various conditions and the amount of live cells and damaged (termed dead) cells were counted. As seen in Figure 5, cells grown in LB as compared to those grown in minimal M9 media (M9) had ~10% less total cell death. When cells were grown in LB and then transferred to M9 media for 0.5 hours of induction there was 3.3% cell death observed; when the cells were grown and induced for 0.5 hours in M9 media there was 17% observed cell death. This indicates that there is less cell damage when cells are grown in LB and then transferred to M9 for induction. Induction times of 1 hour and 1.5 hours caused cell death to increase to 5% and 26% respectively. Induction time was the most influential variable in terms of affecting cell viability. When cells were grown in LB and transferred to M9 media for a 0.5 hour

induction followed by transfer to a deuterated PBS buffer, cell death decreased to 2.3%. These conditions were determined to be optimal.

The second source of protocol optimization was to determine the appropriate method of lysing the cells. Keeping in mind the sample size and what was previously shown to inactivate APH, several different conditions were tried. Figure 6 shows that lanes 3-12 exhibit good cell lysis as seen by the presence of several protein bands as well as an overexpression of APH which is boxed in at 31 kDa. Addition of lysozyme did not significantly increase the amount of cell lysis. The optimal method of lysis was determined to be at least 4 freeze-thaw cycles.

HMQC spectra of whole cells grown and induced under optimal conditions produced a spectrum with 9 distinct peaks (Figure 7). The HMQC spectra of the supernatant did not contain a significant signal indicating that there was little to no leakage of APH out of the cell at this time. The HMQC spectra of the lysate contained an additional 20 peaks, this indicates that once released from the crowded environment of the cell, APH is much more visible. The lysate, while less crowded, still contains all of the proteins and organelles that were once contained in the cell and therefore we do not expect to see a re-establishment of the spectra of purified labeled APH.

In-cell NMR experiments were performed on *E.coli* BL21 (DES) cells containing an empty pET-15b vector as a negative control. In Figure 8, HSQC NMR experiments show that when grown under optimal growth and induction conditions there is some inclusion of ^{15}N into the cell. The supernatant does not have visible ^{15}N signal and the lysate shows a reappearance of the same 4 peaks. This reappearance indicates that there is inclusion of ^{15}N into the cell. Compared to the spectra of our in-cell APH, APH has an increased number of peaks confirming that we are able to detect, although a bit limited by the lack of varying peaks, the labeled APH.

ii. In-cell structural changes of APH

LIVE/DEAD cell assays were used to determine the appropriate amount of antibiotic (neomycin B, tobramycin or kanamycin A) to add to the whole cell sample (Figure 5). The goal was to determine the antibiotic that could be present in high concentrations, without

causing more than 5% cell death. In Figure 5, b-d compare amount of antibiotic added to the number of live and dead cells that resulted. It was concluded that the addition of neomycin B caused less cell death at higher concentrations than either kanamycin A or tobramycin. However, these experiments showed that relatively little aminoglycoside could be used before inducing large amounts of cell death.

In Figure 4, HSQC NMR experiments of APH with 150 mg/ml BSA show that in the presence of a crowding agent, APH is still highly overlapped and therefore flexible. HSQC NMR experiments of the addition of 5 mM neomycin B to APH in the presence of crowding agent BSA resulted in a large amount of peak dispersion (Figure 4). BSA interacts with neomycin, therefore high concentrations were necessary to ensure APH saturation [45]. The peak dispersion indicates that the binding of neomycin B causes a conformational change of APH even when in crowding conditions.

Shown in Figure 7 are spectra of the whole cell, supernatant, lysate and lysate with neomycin. The addition of 10 mM neomycin B to the lysate causes shifts in several resonances, best seen by the overlay image in Figure 7. These shifts tell us that the binding of neomycin B to APH causes a conformational change in the crowded environment of the lysate. The mechanism by which aminoglycosides work to kill bacterial cells makes it difficult to visualize binding AGMEs in the cell. This was shown to be the case with visualizing APH bound to neomycin B in the cell.

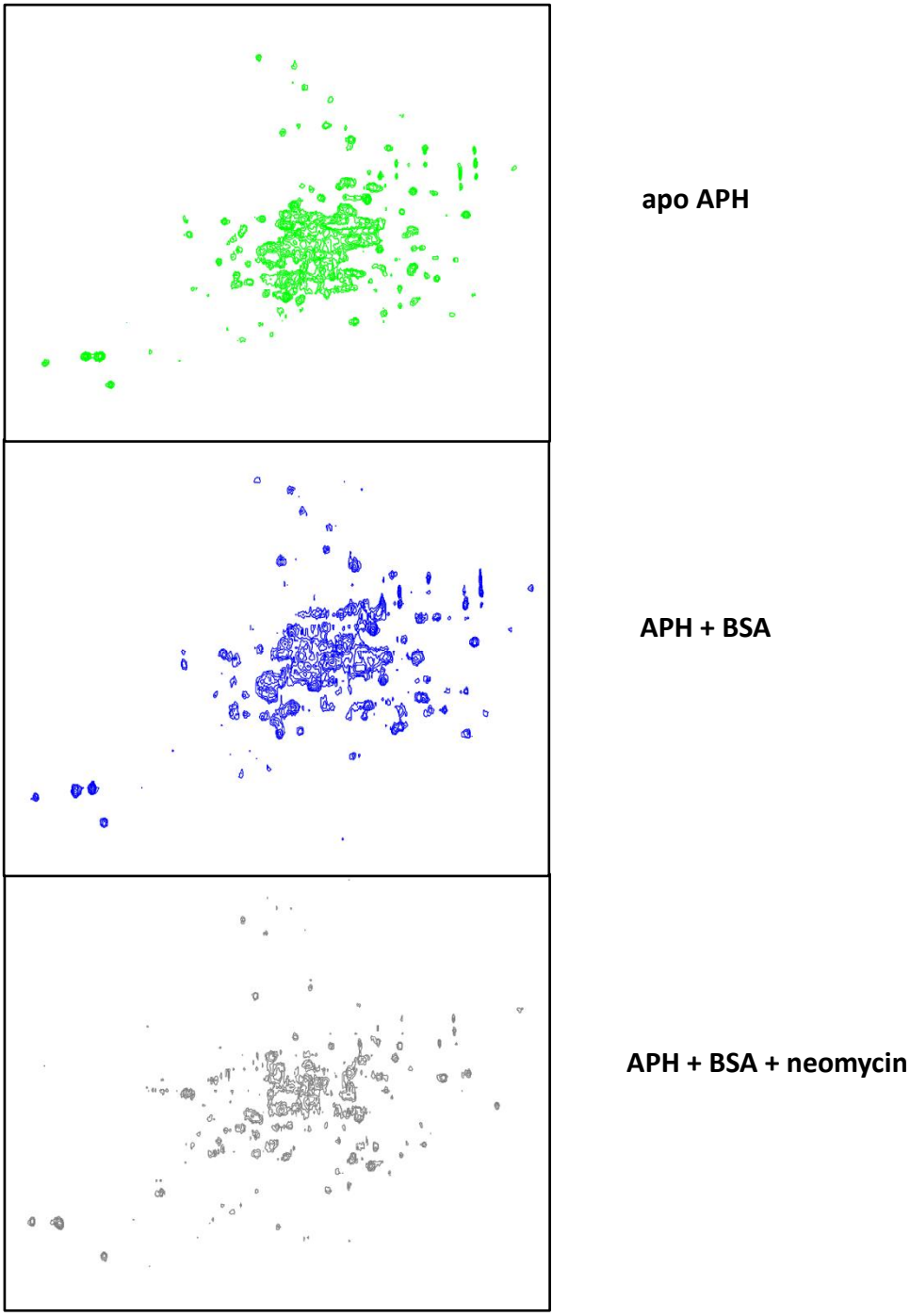


Figure 4: ^{1}H ^{15}N HSQC NMR spectra of APH complexes. APH in its apo (top), in the presence of 150 mg/ml BSA (middle), and in the presence of 150 mg/ml BSA and 5mM neomycin B (bottom) are shown. All spectra were taken under similar environmental conditions and shown to matching contour levels.

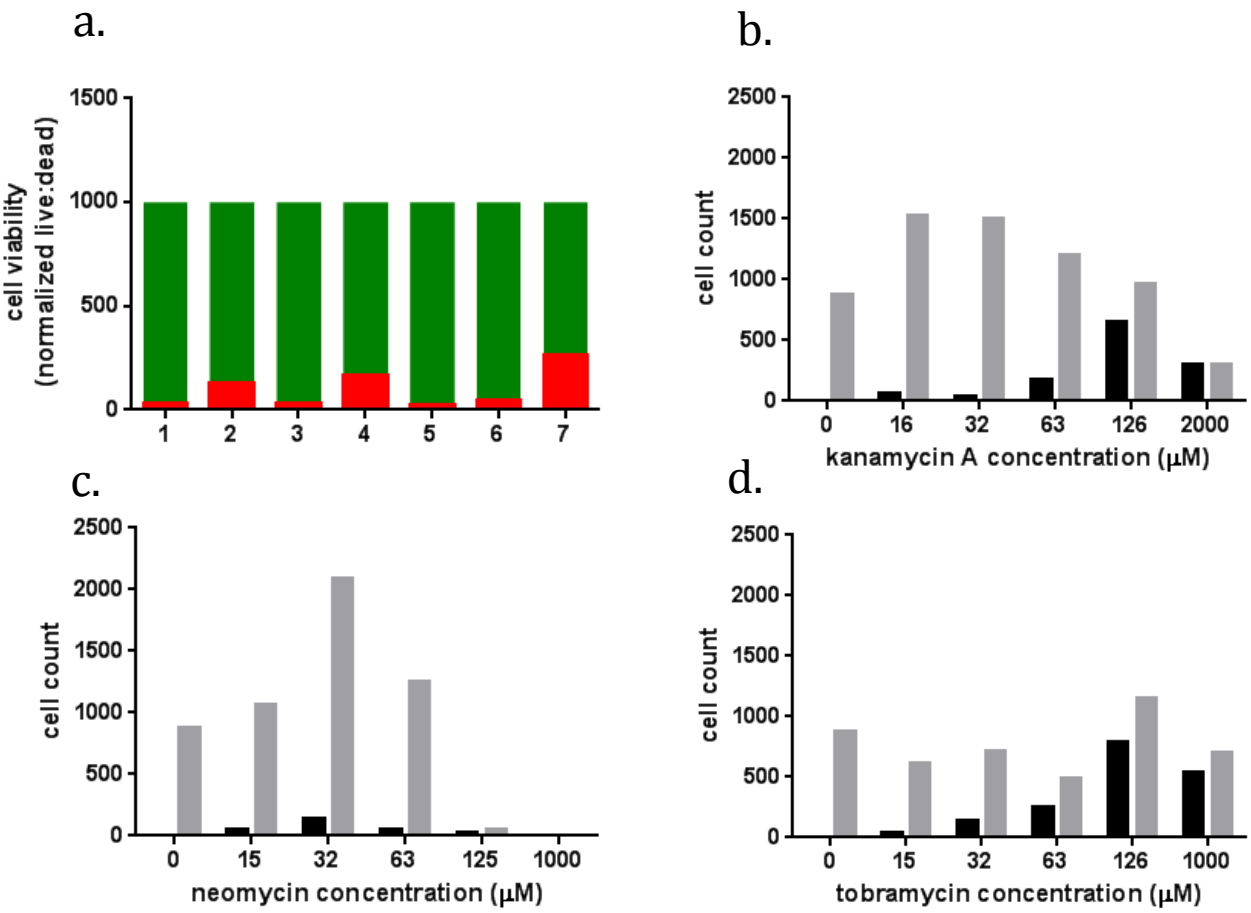


Figure 5: Results of LIVE/DEAD cell assays, (a.) total cell count for each growth condition was normalized to 1000. Green portion represents cells counted as alive, and the red portion represents cells counted as damaged or dead. Growing conditions include cells that were grown in LB media and not induced (lane 1), cells grown in M9 media and not induced (lane 2), cells grown in LB and transferred to M9 for a 0.5 hour induction (lane 3), cells grown in M9 and induced for 0.5 hours (lane 4), cells grown in LB and transferred to M9 for 0.5 hour induction then transferred to PBS buffer (lane 5), cells grown in LB and transferred to M9 for 1 hour of induction (lane 6), and cells grown in LB and transferred to M9 for 1.5 hours of induction. (b-d) LIVE/DEAD cell assays of cells grown and induced for 0.5 hours under optimal growth conditions. Cells were then exposed to various amounts of an aminoglycoside antibiotic: kanamycin A (b), neomycin B (c) and tobramycin (d). After 45 minutes of incubation cells were stained and fluorescence was viewed. Live (light grey) and dead (black) cells were counted from images taken

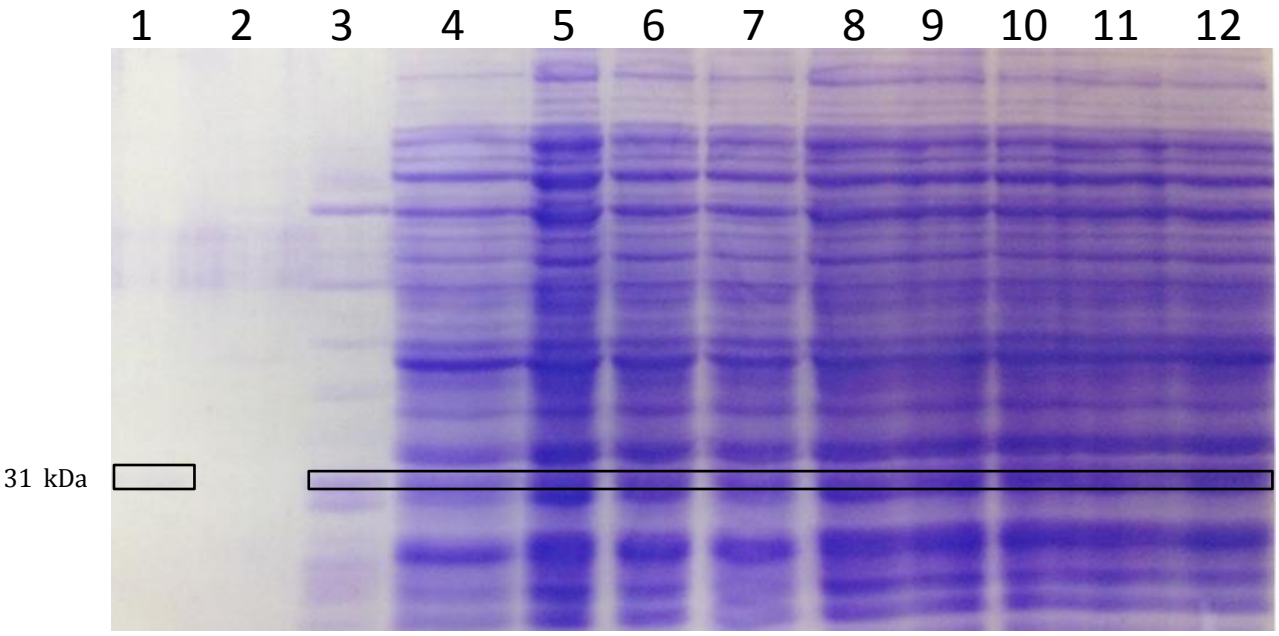


Figure 6: SDS gel picture of proteins extracted using various cell lysis techniques: purified APH (lane 1), cell supernatant prior to lysis (lane 2), freeze thaw 3x with heated lysozyme (lane 3), freeze thaw 3x (lane 4), freeze thaw 3x with unheated lysozyme (lane 5), freeze thaw 3x with preheated lysozyme (lane 6), freeze thaw 4x (lane 7), freeze thaw 4x with heated lysozyme (lane 8), freeze thaw 4x with preheated lysozyme (lane 9), freeze thaw 5x (lane 10), freeze thaw with unheated lysozyme (lane 11), and freeze thaw 5x with preheated lysozyme (lane 12). The black box depicts the location of APH on the gel in lane 1, and in lanes 3-12.

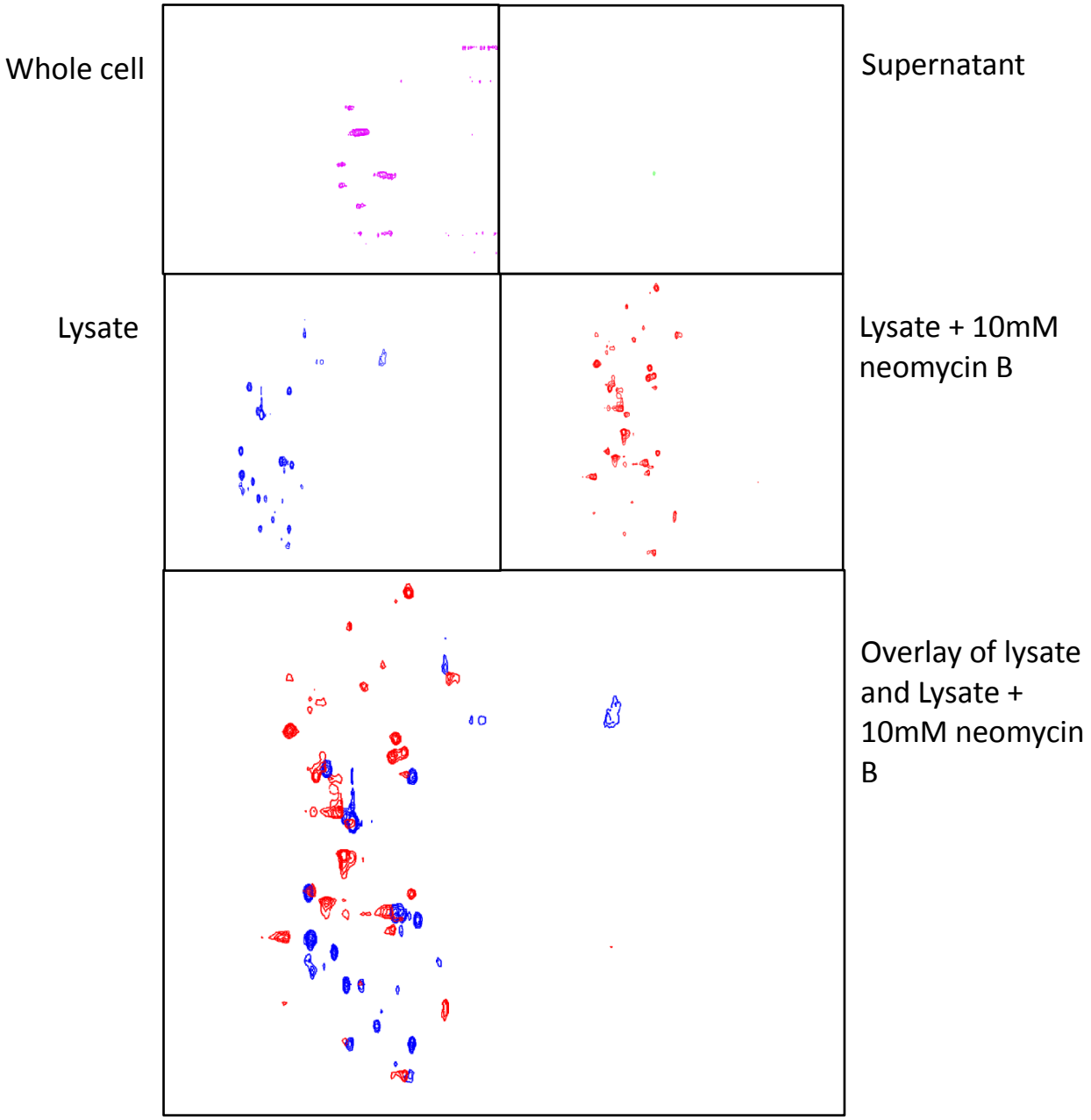


Figure 7: ^{1}H- ^{15}N HMQC NMR spectra of in-cell experiments. APH located in the cell (upper left) is purple, the supernatant (upper right) is green, the lysate (middle left) is blue, lysate plus 10 mM neomycin (middle right) is red and an overlay of spectra with lysate (blue) and lysate with 10 mM neomycin (red) is in the lower panel. All spectra were taken under similar experimental conditions and shown to matching contour levels.

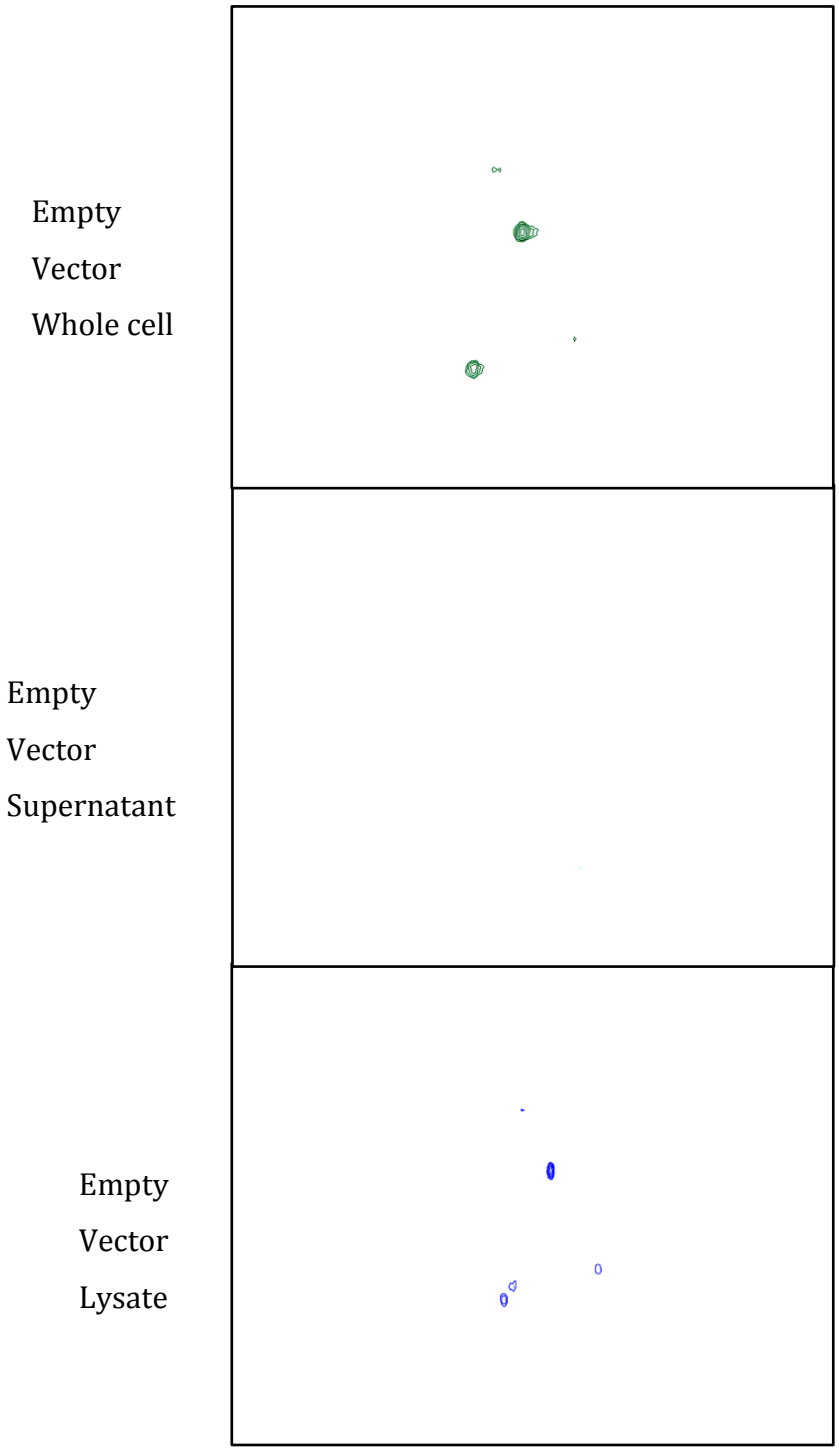


Figure 8: ^{1}H- ^{15}N HMQC NMR spectra of *e.coli* (BL21) cells containing an empty pET-15b vector. Whole cell (top) is shown in green, supernatant (middle) is shown in red, and lysate (bottom) is shown in blue. All spectra were taken under similar experimental conditions and shown to matching contour levels.

Chapter III: APH flexibility allows binding to structurally rigid aminoglycosides

A. Background

i. Introduction to acetyltransferases(3)-IIa and IIIb

Acetyltransferases AAC(3)-IIa and AAC(3)-IIIb will be referred to as AAC-IIa and AAC-IIIb unless specificity is required. APH is a highly promiscuous AGME with a known flexible nature. Aminoglycoside acetyltransferases are another family of AGMEs, and among them they have range of substrate profiles as well as intrinsic disorder. Two well-studied AAC's: AAC-IIa and AAC-IIIb catalyze the transfer of an acetyl group from coenzyme A (CoASH) onto the 3-N position on the central 2-DOS ring of aminoglycoside antibiotics [46]. Modification at this site causes a significant loss of antibiotic effectiveness. AAC-IIa, like APH, is highly dynamic in solution and displays properties of being intrinsically disordered in the absence of aminoglycoside substrate [2]. Upon binding of aminoglycoside, AAC-IIa adapts a well-defined structure (Figure 9). Unlike APH, AAC-IIa has a limited substrate profile, selecting aminoglycosides almost exclusively from the kanamycin family.

AAC-IIIb has a large substrate profile and is able to confer resistance to antibiotics from both the kanamycin and neomycin families; AAC-IIIb does not have structural flexibility in the absence of aminoglycosides. The binding of CoASH to AAC-IIIb causes increased flexibility of the long loop in the antibiotic binding domain [47]. The presence of CoASH causes an increased association between the enzyme and antibiotic for both AAC-IIa and AAC-IIIb [2]. AAC-IIa shares approximately 35% amino acid sequence identity and approximately 39% sequence similarity with AAC-IIIb [2]. There are no crystal structures available for either of these proteins, but structure models show that they are very similar and superimpose to 1.43 Å over the entire protein [2]. The source of differences in their substrate promiscuity is still under investigation.

ii. Binding of sisomicin to acetyltransferases(3)-IIa and IIIb

Sisomicin is an aminoglycoside first isolated in 1970, and is active against gram-positive bacteria [48]. Sisomicin is considered part of the gentamicin family, an aminoglycoside family with a 4,6-disubstituted central 2-DOS ring (Figure 1) [49]. Sisomicin contains an unsaturated diamino sugar ring which is unique to it and netilmicin. Sisomicin contains 2 methyl groups on its double primed ring, which may influence its ability to bind various AGMEs. Netilmicin is identical to sisomicin except for an additional methyl group on its unprimed central ring (Figure 1). Kinetic studies revealed that sisomicin is acetylated at a faster rate by AAC-IIIb but has a lower K_m value with AAC-IIa [2]. Among the aminoglycosides tested with AAC-IIa, sisomicin has the lowest K_m value. ITC experiments reveal that association of sisomicin to AAC-IIa is enthalpically favored (-49 kcal/mol) and entropically disfavored. When sisomicin associates to the binary AAC-IIa-CoASH complex, the aminoglycoside affinity increases 15-50 fold and enthalpy is less favored (-9.7 kcal/mol) [2]. Binding of sisomicin to AAC-IIIb is associated with a favorable enthalpy. For both enzymes, the addition of CoASH causes sisomicin to bind with higher affinity, seen by a decrease in their respective K_D values [2]. The formation of ternary complexes with sisomicin causes an increase in favorable enthalpy with AAC-IIIb but a decrease in favorable enthalpy with AAC-IIa. Changes in enthalpy are compensated by changes in entropy to result in relatively unchanged changes in free energy [2].

Mentioned previously, NMR experiments show that the spectra of apo-AAC-IIa are highly overlapped, indicative of an intrinsically disordered protein. Binding of tobramycin to AAC-IIa causes the complex to gain structure. Binding of sisomicin to AAC-IIa also causes a gain in structure, however when compared to the tobramycin binary complex, there is less peak dispersion indicating that the sisomicin binary complex retains some flexibility (Figure 9). The addition of tobramycin to the AAC-IIa-CoASH complex, shown in Figure 9, reveals that formation of the ternary complex is very similar to that of the tobramycin binary complex. Addition of sisomicin to form the ternary complex causes a larger change in peak dispersion. This indicates that CoASH is required by the AAC-IIa-sisomicin complex to achieve similarly well-defined structural features similar to that observed with the binary AAC-IIa-tobramycin and ternary AAC-IIa-CoASH-tobramycin complexes [2]. AAC-IIa may

be inhibited from entering a more structured form when only sisomicin binds because of the rigid diamino sugar ring. To investigate the ability of flexible proteins to overcome structural differences in substrates, the binding interactions of APH are examined with sisomicin and netilmicin.

iii. Formation of differing ternary complexes dependent upon order of addition

AAC-IIIb with its two substrates, CoASH and aminoglycosides, forms a ternary complex. However, adding the substrates, neomycin B and paromomycin, in varying orders results in ternary complexes that are not identical to one another (Norris, unpublished). In the first pathway to form the ternary complex the binding order is AAC-IIIb, neomycin then CoASH, in the second pathway the order of binding is AAC-IIIb, CoASH and then neomycin. However, Hess's law is still obeyed in the formation of the ternary complex in both forms [50]. Hess's law states that "the enthalpy change for any sequence of reactions that sum to the same overall reaction is identical" [51]. Based on Hess's law, the change in enthalpy found by adding the substrates in differing orders should result in the same total change in enthalpy if the same ternary product is formed. Using differential scanning calorimetry (DSC) they demonstrated that the melting temperature of ternary complex AAC-CoASH-neomycin was 2.3 °C higher than the melting temperature of ternary complex AAC-neomycin-CoASH. There are also differences in the hydrodynamic radius, final NMR spectra, and solvent protection of the ternary complexes dependent upon the order of addition (Norris *et al.*, manuscript under review). Together the data suggest that the order of addition plays a large role in the final ternary complex that is formed with AAC-IIIb. This is the first time that the order of addition has been investigated with AGMEs. Similar differences were observed with AAC-IIa and sisomicin (Norris, unpublished). Here the order of addition is further investigated for APH by DSC as well as ITC.

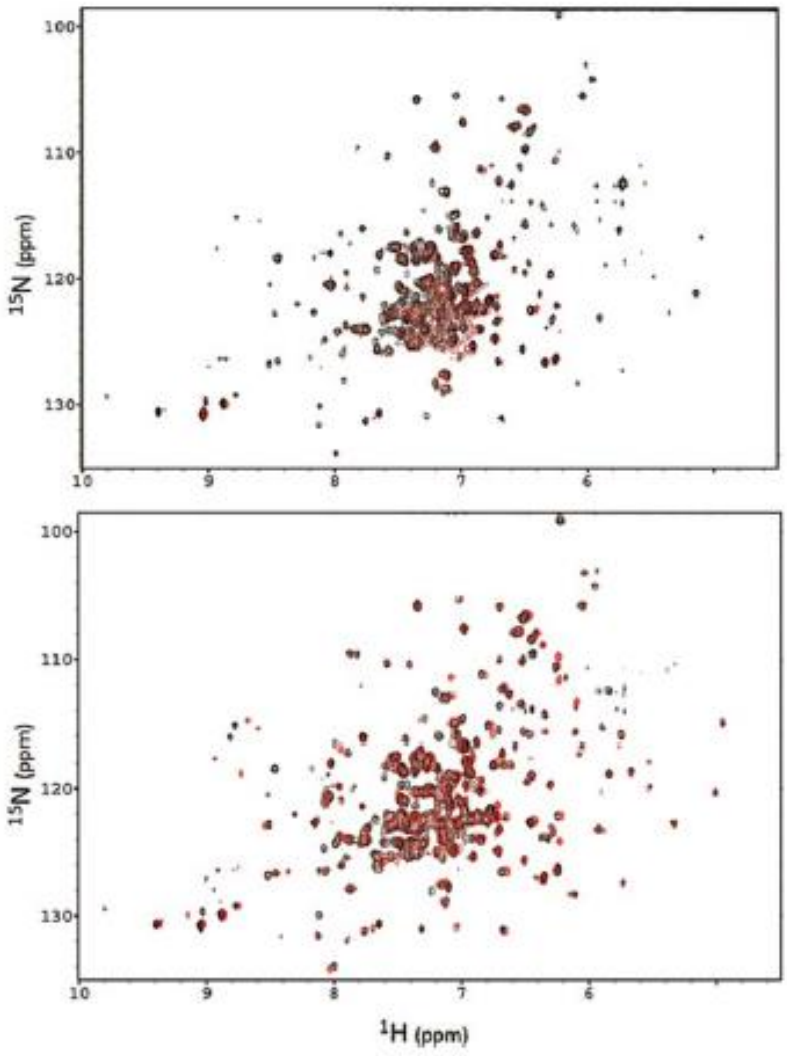


Figure 9: NMR spectra comparing the peak dispersion of binary (top) and ternary (bottom) complexes of sisomicin (red) and tobramycin (black) with AAC-IIa. Reprinted with permission [2].

B. Methods

i. Chemicals and Reagents

99% D_2O and ^{15}N-enriched salts were purchased from Cambridge Isotope Laboratories (Andover, MA). Thrombin was purchased from Enzyme Research Laboratories (South Bend, IN), IPTG from Inalco Spa (Milan, Italy) and the high performance Ni Sepharose resin used for APH purification was purchased from Amersham biosciences (Piscataway, NJ). Ion-exchange matrix Macro Q is from Bio-Rad laboratories (Hercules, CA). Aminoglycoside, and all other chemicals and reagents were purchases in the highest purity available from Sigma-Aldrich or Fisher. Desulfated Aminoglycoside were used for all kinetic and thermodynamic studies, concentrations were determined by activity assays previously described [52].

ii. Growth and purification of APH

Following a previously established protocol, BL21 *E.coli* cells with APH containing pET-15b expression vector were grown at 37 °C with agitation to an OD_{600} of ~0.8 in either LB (for unlabeled APH) or M9 minimal media containing $^{15}NH_4Cl$ (for ^{15}N labeled APH) [30, 36]. LB contained 0.1 mg/ml AMP. APH expression was induced by the addition of 1 mM of IPTG. Cells were harvested by centrifugation after 4 hours, and stored at -80 °C for up to 12 months. For purification, cells were suspended in lysis buffer (100 mM NaCl, 20 mM imidazole, 200 μM PMSF, and 50 mM Tris-HCl pH 7.4 at 4 °C). Cells were lysed by three passes through a French press and cell debris pelleted by centrifugation. APH was purified from the crude lysate by nickel affinity chromatography. Thrombin was used to proteolytically remove the Histag from APH. Separation of cleaved APH was achieved through nickel affinity chromatography, and separation from excess thrombin by ion-exchange chromatography. The ratio of UV absorbance at 280 nm and 260 nm confirmed that the protein was freed from nucleic acids. Purified APH was dialyzed extensively in appropriate buffer at 50 mM (pH 7.4) at 4 °C, 100 mM NaCl, and 2 mM TCEP-HCl, then stored at 4 °C for up to one week or frozen immediately using liquid nitrogen and stored at -80 °C. Final concentrations of protein were determined at absorbance of 280 nm using an extinction coefficient value of 1.54.

iii. Steady-state kinetics

Sisomicin does not have a hydroxyl located on its C-3 primed ring, therefore APH is unable to chemically modify sisomicin. Kinetic parameters for the inhibition activity of sisomicin were determined by using a continuous assay previously described [36]. Phosphorylation of aminoglycoside antibiotics is monitored by a coupled reaction of the ADP generated from phosphorylation of the aminoglycoside to the oxidation of NADH using the enzymes pyruvate kinase and lactate dehydrogenase. The oxidation of NADH is monitored at 340 nm using a Cary-Win UV-vis spectrophotometer (Varian, Palo Alto, CA). The spectrometer was blanked with 985 µl deionized water, and the NADH stock was tested by adding 15 µl to water and observing the change in absorbance. Next, 970 µl of assay mix (50 mM Tris pH 7.4, 50 mM KCl, 1 mM ATP, 1.5 mM $MgCl_2$, and 2 mM phosphoenolpyruvate trisodium salt at 25 °C) is added to appropriate amounts of sisomicin and kanamycin A as well as 150 µM NADH and 0.02 mg/ml pyruvate kinase/lactate dehydrogenase enzyme solution. The reaction was then initiated by the addition of 10 µl of 100 µM purified APH. The reactions followed Michaelis-Menten type kinetics where sisomicin is a competitive inhibitor. The specific activity (micromoles per second per milligram) was plotted versus substrate concentration and fitted to the equation below in order to determine the K_i of sisomicin,

$$v = (V_{\max}[S])/(K_m + [S] + \frac{[S]^2}{K_i})$$

where ν=the initial velocity, and K_m is the Michaelis constant.

iv. Isothermal titration calorimetry

ITC experiments were performed at 25 °C using a VP-ITC macrocalorimeter from Microcal, Inc. (Northampton, MA). APH concentrations were kept between 20-30 µM to maintain the c-value, a parameter obtained by multiplying the association constant and the total concentration of the ligand binding site, was kept between 1 and 100. Measurements were carried out in 50 mM Tris-HCl, PIPES, HEPES, or ACES buffers which also contained 100 mM NaCl and 2 mM TCEP-HCl at a pH of 7.4. Enzyme preparations include a final step of dialysis into one of the listed buffers. Ligand solutions were prepared with the same dialysate as was used for the enzyme. The pH was checked for both solutions and kept

within 0.05 units of each other, samples were then degassed under vacuum for 10 minutes before being appropriately loaded into the VP-ITC macrocalorimeter. Titrations of substrate into enzyme solution consisted of 29 injections of 10 µl, separated by 240 seconds with a cell stirring speed of 300 rpm.

Binary titrations included the titration of aminoglycoside, or AMPPCP solution into enzyme solution. Aminoglycoside concentrations ranged from 0.25-1 mM, and the AMPPCP concentration was 2.25 mM. Ternary titrations included either the titration of aminoglycoside into the enzyme-Mg-AMPPCP complex, or the titration of AMPPCP into enzyme-aminoglycoside-Mg complex. In ternary experiments where aminoglycoside was titrated in, the Mg-AMPPCP concentration was kept constant at 1.25 mM in both solutions. In ternary experiments where AMPPCP was titrated in, the antibiotic concentration was kept constant at either 0.5 or 1 mM for either sisomicin or netilmicin respectively, and Mg was at saturating levels of 1.25 mM. By keeping all of the additional substrates at saturating levels in both solutions the heat associated with binding of either aminoglycoside or AMPPCP respectively were measured exclusively. Enzymatic activity was periodically checked before and after titrations. Sedphat software as well as nitpic software were used to fit the data. Isotherms depicted were created using nitpic software. Binding of an aminoglycoside to APH causes a well-documented shift in the pK_a values of several functional groups, therefore each binding experiment was performed in at least 3 of the following buffers: Tris-HCl, ACES, HEPES, or PIPES. The buffers have varying heats of ionization (ΔH_{ion}), 11.4, 7.3, 4.87, and 2.7 respectively [53]. The observed enthalpy (ΔH_{obs}) contains contributions from various sources as seen by the equation [54]:

$$\Delta H_{obs} = \Delta H_{int} + \Delta n[\alpha \Delta H_{ion} + (1 - \alpha \Delta H_{enz})] + \Delta H_{bind}$$

In the equation above, ΔH_{int} is the intrinsic enthalpy of binding, and Δn is the net protonation. The portion of the equation in brackets represents the heat of ionization from the buffer and the protein (ΔH_{enz}) which maintains the pH. In the presence of high concentrations of salt (i.e., 100 mM NaCl) the heat of binding of buffer to enzyme (ΔH_{bind}) is assumed to be zero [54]. Therefore by performing each binding experiment in 3 buffers with different ΔH_{ion}, the ΔH_{int} and Δn can be determined using the equation:

$$\Delta H_{obs} = \Delta H_{int} + \Delta n * \Delta H_{ion}$$

v. Differential scanning calorimetry

DSC experiments were performed in PIPES buffer on a VP-DSC Microcalorimeter from MicroCal. It was previously established that APH is able to refold after heat denaturation. The melting transition data was recorded from 10 °C until 75 °C for just the buffer, apo APH, binary APH-Sisomicin, ternary complexes where sisomicin was added to APH-Mg-AMPPCP complex or AMPPCP was added to APH-sisomicin-Mg complex and buffer with Mg, sisomicin and AMPPCP. PIPES buffer was used in the reference cell. All samples were degassed for 15 minutes prior to injection and contained one to three of the following: 50 µM purified APH dialyzed in PIPES buffer (50 mM PIPES, 100 mMNaCl, 2 mM T-CEP and pH of 7.4), 1.25 mM $MgCl_2$, 1.25 mM AMPPCP, 0.5 mM sisomicin, with the final volume made up of PIPES buffer. Origin software was used to analyze the data with a non-2-state model for fitting. Baselines were not stable enough to reliably calculate the change in heat capacity.

vi. Nuclear magnetic resonance

NMR samples used contained 150 µM purified ^{15}N labeled APH protein, in 50 mM MOPS buffer, 2 mM TCEP-HCl, 100 mM NaCl, and 7% D_2O, pH 7.4. Experiments included using samples of apo APH, the addition of 0.5mM desulfated sisomicin, and finally the addition of 1.25 mM $MgCl_2$ and 1.25 mM AMPPCP. Apo APH sample was transferred to a Shigemi tube (Allison Park, PA) with a total volume of 350 µl. HSQC spectra were obtained on a Varian Inova 600 MHz triple resonance spectrometer at 25 °C at the University of Tennessee. HSQC experiment parameters were optimized, and included a delay of 1.5 seconds between scans, pulse width of 8.05 µs, 64 transients, and a spectral width of 8012. The binary and ternary samples were prepared by titration of appropriate amount of substrate into apo APH sample, HSQC parameters were kept the same. Spectra were processed with nmrDraw and exported to Sparky for analysis and display [43, 44]. Adobe Photoshop software was used to invert and change the color of the images. APH protein model 1L8T from the protein data bank was used to highlight shifted amino acids in Molecular Operating Environment (MOE) at The University of Tennessee. The model is from crystal structure analysis of APH bound to ADP and kanamycin A [27].

C. Results/Discussion

i. Kinetic interactions of APH with sisomicin

Most aminoglycoside substrates demonstrate substrate inhibition as they compete for the same binding site and sisomicin is not an exception [2, 36]. However because sisomicin does not have a hydroxyl group on its 3′ carbon, it is unable to be chemically modified by APH. As expected, it is a competitive inhibitor with respect to aminoglycosides and the determined K_i value of sisomicin is 0.203 ± 0.089 mM. Sisomicin has an inhibition constant (K_i) of >700 μM and ~1000 μM with AAC-IIIb and AAC-IIa respectively. It is important to note that K_i and K_m values are not correlated to one another. For instance, a substrate with a low K_m value need not have a low K_i value. Therefore, no further conclusions can be drawn from this value.

ii. Thermodynamic interactions of APH with sisomicin and netilmicin

Binary and ternary thermodynamic interactions of APH with kanamycin A, kanamycin B, tobramycin, amikacin, ribostamycin, neomycin B, paromomycin I, and lividomycin A were previously published in 2004 [30]. The previous ITC experiments were done at 37 °C, contained 50-100 μM APH, 0.75-3 mM aminoglycoside concentration and buffers contained 100 mM KCl instead of 100 mM NaCl. However, these changes should not affect the observed trends [30]. Furthermore, binary APH ITC experiments were performed under currently used conditions with antibiotics: kanamycin A, kanamycin B, neomycin B and ribostamycin (Wright, unpublished data). At 25 °C, antibiotics have similar K_D values to previously published K_D values, less favorable enthalpy (ranging from 3 to 29.8 kcal/mol less favorable due to large heat capacity change observed with this enzyme), and a correlating increase in favorable entropy. Binary binding parameters for APH complexes with sisomicin, netilmicin and AMPPCP are found in Table 1. Binary binding of APH with sisomicin had a K_D value similar to that of kanamycin A. Kanamycin B, neomycin B, paromomycin I, lividomycin A, ribostamycin and tobramycin all bind to APH with stronger affinities than sisomicin and netilmicin [30]. However, both sisomicin and netilmicin bind with stronger affinities than amikacin, which has a bulky group attached to the N-1 of its 2-DOS ring. The neamine portion of the antibiotic has been shown to be important for

binding; therefore large groups found on the first two rings may be more inhibitory than the unsaturated prime diamino ring found on sisomicin and netilmicin. Netilmicin has a K_D value approximately two fold higher than that of sisomicin. This difference can be attributed to the additional methyl group located on netilmicin in the same location that amikacin has its bulky group (Figure 1). This methyl group is predicted to give netilmicin an increased hydrophobic property.

Previous ternary experiments performed in 2004 with APH included changes already mentioned as well as the use of $CaCl_2$ and ATP instead of $MgCl_2$ and AMPPCP [30]. Ternary parameters determined by ITC are found in Table 2. The K_D value of sisomicin to the APH-Mg-AMPPCP complex showed little change from binary K_D value, similar to previous results where the addition of antibiotic to APH-Ca-ATP complex remained similar to the binary K_D, or slightly decreased [30]. This is unlike what is seen with enzyme AAC-IIIb, where the addition of co-substrate causes a great increase in affinity of the antibiotic for the enzyme complex [46]. Addition of co-substrate has been shown to increase affinity of aminoglycoside for enzymes, APH, AAC-IIIb, AAC-IIa, ANT(2″)-Ia, and AAC(6′)-Iy [2, 30, 49, 55]. Sisomicin follows this trend seen by its general lower K_D value when binding the APH-MgAMPPCP complex, whereas netilmicin did not.

Interestingly, binding of netilmicin or sisomicin to APH is associated with relatively less favored enthalpy, as well as the most favorable entropy seen in literature of APH relative to other aminoglycosides [30]. Formation of the netilmicin binary complex had the most unfavorable intrinsic enthalpy, and the sisomicin binary complex was only slightly more favorable: -7.6 and -10.3 kcal/mol, respectively (Table 1). Binary experiments, APH-sisomicin, performed in Tris-HCl, and HEPES buffers had a favorable entropy (18 and 5.8 cal/K respectively) associated with the binding of sisomicin to APH (Figure 10). Binary Netilmicin ITC experiments had a favorable entropic contribution in all buffers (Figure 11). Netilmicin has the most favorable entropy associated with binary complex formation of an aminoglycoside with APH as reported so far in literature. Netilmicin binary complex formation in Tris-HCl buffer was endothermic because of proton contribution of the buffer, and low enthalpic contributions of the reaction (Figure 11). Favorable entropy is often a reflection of increased disorder caused by the release of water [31]. There is compensation

that occurs with enthalpy and entropy values to yield a relatively unchanged favorable ΔG. The additional methyl group on netilmicin seems to also play a role in the thermodynamic contributions of binding, further emphasizing trends seen with sisomicin. The hydrophobic qualities of these substrates cause an increase in favorable entropic contributions as well as a correlated decrease in favorable enthalpic contributions. This indicates that there is interaction of the hydrophobic groups with APH's active site, as was seen with AAC(6′)-Iy [55]. APH is able to interact with the double primed ring region of the antibiotics and methyl groups found here, which affects the order of water molecules and various global hydrogen bonds formed.

Formation of the binary APH complexes with sisomicin and netilmicin are both associated with a positive net protonation of the complex, which may indicate an upshift in pK_a values for several functional groups in both ligand and enzyme (Figure 12) [54, 56]. Amikacin and ribostamycin are the only antibiotics recorded to cause a net deprotonation when binding APH [30]. There is also positive net protonation associated with the addition of sisomicin or netilmicin to the APH-Mg-AMPPCP complex. This follows the general trend seen from previous experiments done with other antibiotics [30]. Binding of aminoglycoside antibiotic to the binary APH-metal-ATP complex has been shown to always have a positive net protonation.

When comparing changes in thermodynamics between the binding of antibiotic to APH (binary) and the binding of antibiotic to APH-metal-ATP complex (ternary) typically the ternary complex has a less favorable enthalpy (10-20 kcal/mol) and an increased favorable entropy [30]. The binding of amikacin is the only antibiotic that has been previously found to cause an increased favorable enthalpy with the formation of the ternary complex [30]. Binding of sisomicin to form the ternary complex had a very slight increase in favorable intrinsic enthalpy (0.2 kcal/mol), whereas binding of netilmicin to form the ternary complex decreased the favorable enthalpy by 1 kcal/mol (Table 2). The reasons behind this have yet to be elucidated at this time. Sisomicin and netilmicin bind fairly tightly with APH yet they do not follow the thermodynamic trends previously seen with this enzyme. The only other antibiotic to deviate from the general thermodynamic trends, amikacin, has the lowest binding affinity to APH, approximately 20 times lower than sisomicin.

Typical carbohydrate-protein interactions are characterized by a favorable enthalpy and unfavorable entropy [57]. Expanding our comparison to other AGMEs, binary binding of sisomicin to AAC-IIIb also yields a small favorable heat contribution made by enthalpy and has a favorable entropy [2]. Binding of sisomicin to AAC-IIa had a highly favorable enthalpic contribution and unfavorable entropic contribution similar to data of binding of other antibiotics to AAC(3)-IIa. Binary binding of netilmicin with AAC(6′)-Iy also has a favorable entropy, however binding of sisomicin did not [55]. The only other antibiotics with documented favorable entropic contribution are kanamycin A binding to either AAC-IIa or IIIb, and amikacin to AAC(6′)-Iy [2, 46, 55]. The reasons behind this similarity are still unknown at this time. Binding of aminoglycosides to AGMEs typically results in favorable enthalpy and unfavorable entropy, additionally seen with AAC(3)-IV, ANT(4′) and ANT(2″) [49, 58, 59].

iii. Thermodynamics of the ternary complex formation are not dependent upon the order of addition

The formation of ternary complex APH-siso-Mg-AMPPCP is associated with a favorable intrinsic enthalpy, and unfavorable entropy (Table 2). The binary complex, APH-AMPPCP, had a favorable enthalpy as well as favorable entropy, consistent with APH binding to other ATP analogs (Table 1) [60]. According to Hess's law the total enthalpy change of one pathway should be the same as another if the same final product is formed. Therefore by adding the enthalpies of binary APH-siso complex and ternary APH-siso-Mg-AMPPCP complex and comparing the total to the total enthalpy found by the adding enthalpy of binary APH-AMPPCP complex to ternary APH-Mg-AMPPCP complex, inferences can be made about the final complex formation dependent upon the order of substrate addition.

$$\Delta H_{obs\ AGME+antibiotic} + \Delta H_{obs\ AGME-antibiotic+nucleotide} = \Delta H_{obs\ AGME+nucleotide} + \Delta H_{obs\ AGME-nucleotide+antibiotic}$$

For ITC, experiments done in Tris-HCl buffer, the total changes in enthalpy for each pathway were within error of each other. This indicates that for APH, the order of binding does not change the thermodynamic properties of the final ternary complex, and therefore follows Hess's law.

iv. Differential scanning calorimetry of APH complexes

As seen in Figure 13, the melting temperature of APH complexes occurred as a single denaturation event (single peak). The T_m of the apo APH was calculated to be 47.5 °C. The T_m of the binary APH-siso complex was 54.2 °C. When compared to previous DSC experiments of APH bound to various well known aminoglycosides substrates, the melting temperature of APH-siso is comparable with that of APH-KanA (Wright, unpublished). This suggests that APH is able to bind sisomicin with a formation of structure similar to that seen with other aminoglycosides. The T_m of ternary APH-siso-Mg-AMPPCP complex and ternary APH-Mg-AMPPCP-siso complexes were 55.2 °C and 54.9 °C respectively. The melting temperatures of both ternary complexes are within 0.3 °C of each other; this indicates that the complex formed by the addition of sisomicin to the APH-Mg-AMPPCP complex is very similar if not identical to the complex formed by the addition of AMPPCP to the APH-sisomicin-Mg complex.

The addition of sisomicin to APH resulted in a higher T_m when compared to the apo APH complex, this is similar to what was seen with other aminoglycosides. This is unlike AAC-IIa which adopts a more flexible conformation to accommodate the methyl groups as well as the unsaturated primed diamino sugar ring of sisomicin, and had a lower T_m than when bound to other aminoglycosides.

v. Nuclear magnetic resonance of APH-siso complex

It was previously shown that even after the binding of sisomicin to flexible protein AAC-IIa, AAC-IIa retained some of its flexibility as compared to its binding of tobramycin [2]. Shown in Figure 14 is the binding of sisomicin to APH, binding results in a peak dispersion that is relatively similar to APH bound to tobramycin (Figure 3). This indicates that the APH conformation formed by sisomicin binding to APH is not drastically different than that of the complex formed by tobramycin binding to APH. The NMR resonances for tobramycin bound APH were previously assigned and published, therefore chemical shifts of specific amino acids can be determined by spectral comparisons [29]. Figure 15 depicts the amino acids that show significant changes in their chemical shifts. Comparison between two-dimensional HSQC spectra of APH-tobramycin complex and APH-sisomicin complex

revealed that there was a significant shift in 23 amino acid assigned resonances. Notably, there was a shift in Glu160 and Asp190. Both amino acids have been shown to interact with the aminoglycoside substrate by x-ray crystallography[27]. There was a noticeable shift in several amino acids in the flexible binding loop that is predicted to be intrinsically disordered: Ala141, Asp144, Asp153, Asp155, Cys156, and Glu160; as well as several other amino acids located in and around the aminoglycoside binding pocket. Out of the 23 amino acids that shifted their resonance, 8 were negatively charged, and 7 were hydrophobic. The fact that amino acid residues showed significant shifts distributed all over the protein, including remote sites, is again consistent with the role of flexibility of APH to bind structurally different aminoglycosides.

Overall the NMR data indicates that the binary APH-sisomicin complex has gained a significant amount of structure as compared to the apo APH complex. The retained flexibility that was observed with AAC-IIa bound to sisomicin is not observed with APH bound to sisomicin. Therefore APH is able to compensate for the additional restrictions presented by sisomicin. The flexible nature of APH is better able to overcome structural differences in substrates to form additional interactions with the substrate. The flexible nature of AAC-IIa seems to have limited interaction even with substrates that it binds fairly well.

Table 1: Thermodynamic parameters for Aminoglycoside binding (binary complex)[a]

aminoglycoside	buffer	K_D (μM)	ΔH_{obs} (kcal/mol)	ΔH_{int} [b] (kcal/mol)	-TΔS (kcal/mol)	ΔG (kcal/mol)	Δn
sisomicin	Tris-HCl	4.7 ± 2.2	-1.9 ± 0.6	-10.4 ± 0.8	-5.4 ± 0.7	-7.3 ± 0.2	0.7 ± 0.1
	HEPES	1.6 ± 0.9	-6.2 ± 0.1		-1.7 ± 0.2	-7.9 ± 0.05	
	PIPES	4.2 ± 1.2	-8.8 ± 0.1		1.5 ± 0.1	-7.3 ± 0.02	
netilmicin	Tris-HCl	7.1 ± 0.7	1.6 ± 0.04	-7.6 ± 0.8	-8.6 ± 0.01	-7.02 ± 0.05	0.8 ± 0.1
	ACES	7.4 ± 1.9	-1.3 ± 0.08		-5.7 ± 0.2	-7.0 ± 0.1	
	HEPES	6.9 ± 0.9	-4.5 ± 0.1		-2.6 ± 0.2	-7.04 ± 0.2	
	PIPES	9.1 ± 0.3	-5.1 ± 0.04		-1.8 ± 0.06	-6.9 ± 0.02	
AMPPCP	Tris-HCl	12.2 ± 8.6	-4.2 ± 2.2	ND	-2.5 ± 2.6	-6.7 ± 0.3	ND

[a] Given errors were calculated by fits to sedphat critical chi-square for error surface projections. [b] Errors for intrinsic enthalpy(ΔH_{int}) and net protonation (Δn) are derived from the deviation from linearity of ΔH_{obs} vs ΔH_{ion} curves. ND stands for 'not determined', since accurate values of ΔH_{int} could not be obtained.

Table 2: Thermodynamic parameters for Aminoglycoside binding (ternary complex)[a]

aminoglycoside	buffer	K_D (μM)	ΔH_{obs} (kcal/mol)	ΔH_{int} [b] (kcal/mol)	-TΔS (kcal/mol)	ΔG (kcal/mol)	Δn[b]
sisomicin	Tris-HCl	4.3 ± 0.6	-5.0 ± 0.6	-10.5 ± 0.5	-2.3 ± 0.4	-7.3 ± 0.1	0.5 ± 0.07
	HEPES	3.2 ± 0.3	-7.8 ± 0.2		0.3 ± 0.3	-7.5 ± 0.05	
	PIPES	4.2 ± 0.08	-9.5 ± 0.05		2.2 ± 0.05	-7.3 ± 0.01	
netilmicin	ACES	27.5 ± 18.8	-3.0 ± 0.7	-6.5 ± 1.9	-3.0 ± 1.2	-6.2 ± 0.5	0.4 ± 0.4
	HEPES	11.0 ± 2.5	-5.4 ± 0.3		-1.4 ± 0.4	-6.8 ± 0.1	
	PIPES	12.3 ± 2.8	-4.9 ± 0.05		-1.8 ± 0.08	-6.7 ± 0.02	
AMPPCP[c]	Tris-HCl	91.5 ± 16.8	-11.8 ± 1.3	-6.4 ± 0.5	6.3 ± 1.1	-5.5 ± 0.07	-0.5 ± 0.06
	HEPES	69.3 ± 3.9	-9.0 ± 1.3		3.3 ± 1.4	-5.7 ± 0.07	
	PIPES	86.6 ± 14.2	-7.4 ± 0.6		1.9 ± 0.7	-5.5 ± 0.05	

[a] Given errors were calculated by fits to sedphat critical chi-square for error surface projections, ternary experiments where the aminoglycoside was titrated into APH-Mg-AMPPCP complex. [b] Errors for intrinsic enthalpy(ΔH_{int}) and net protonation (Δn) are derived from the deviation from linearity of ΔH_{obs} vs ΔH_{ion} curves. [c] ternary experiments where AMPPCP was titrated into APH-sisomicin-Mg complex.

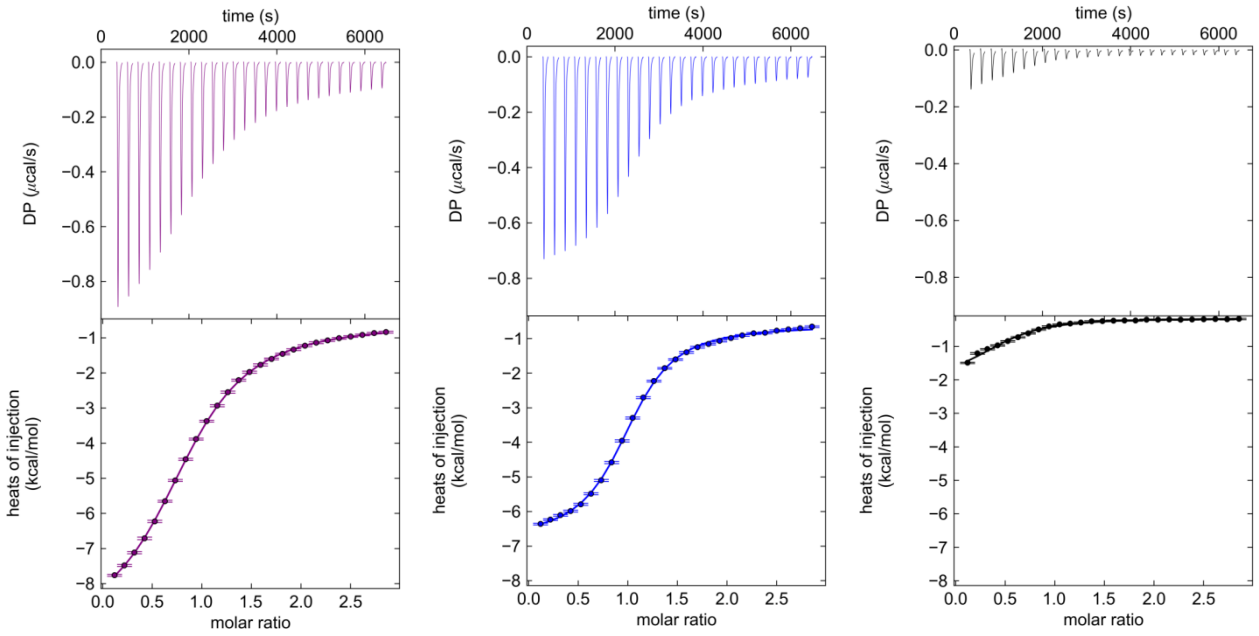


Figure 10: Typical thermogram (top) and isotherm (bottom) for titration of sisomicin into APH in buffers PIPES (purple), HEPES (blue) and Tris-HCl (black). Time integration of the thermal power yields the heat of injection. In the isotherms, data points are shown with a fitted line to single-site binding. Scale of y-axis is matched in all isotherms for the ease of visual comparison.

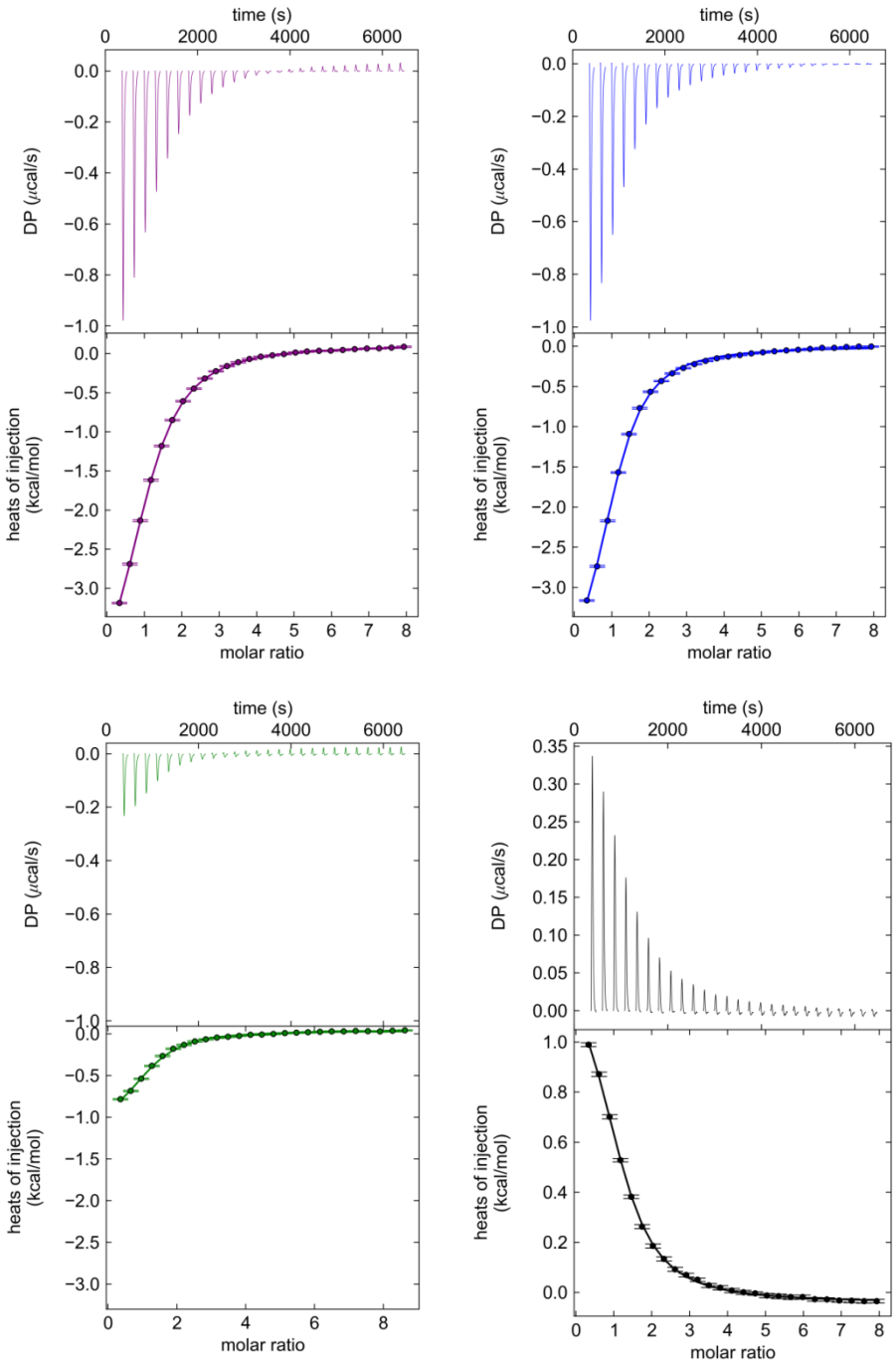


Figure 11: Typical thermogram (top) and isotherm (bottom) for titration of netilmicin into APH in buffers PIPES (purple), HEPES (blue), ACES (green) and Tris-HCl (black) Time integration of the thermal power yields the heat of injection. In the isotherms, data points are shown with a fitted line to single-site binding.

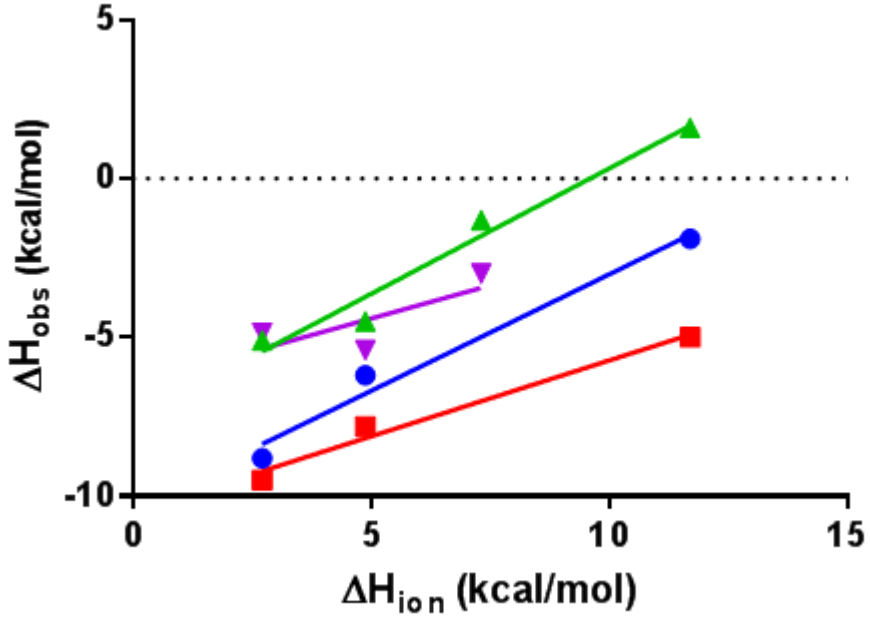


Figure 12 : Determination of the intrinsic enthalpy of binding. The observed enthalpy determined in different buffers is plotted vs the heat of ionization of the buffer. Depicted are binary APH-sisomcin (blue), ternary APH-Mg-AMPPCP-sisomcin (red), binary APH-netilmicin (green), and ternary APH-Mg-AMPPCP-netilmicin (purple). R values for the linear regressions are >0.95, except ternary APH-Mg-AMPPCP-netilmicin which had an R value of .58.

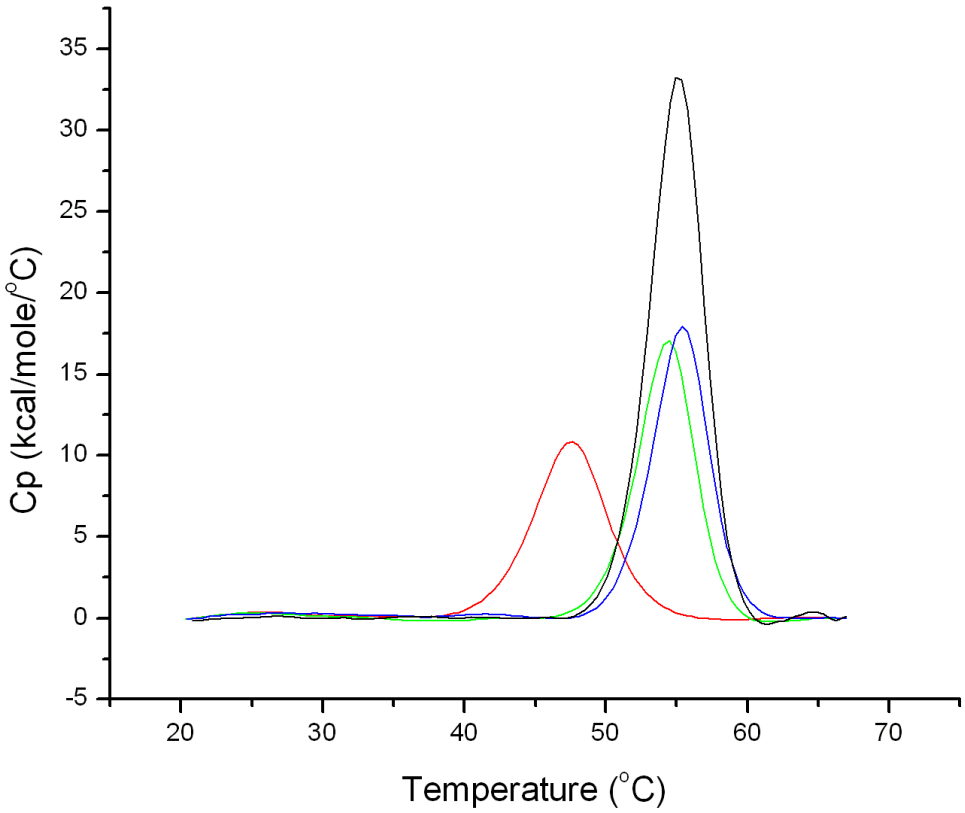


Figure 13: DSC traces of APH complexes apo (red), binary APH-sisomicin (green), ternary APH-Mg-AMPPCP-sisomicin (black), and ternary APH-sisomicin-Mg-AMPPCP (blue) are shown above.

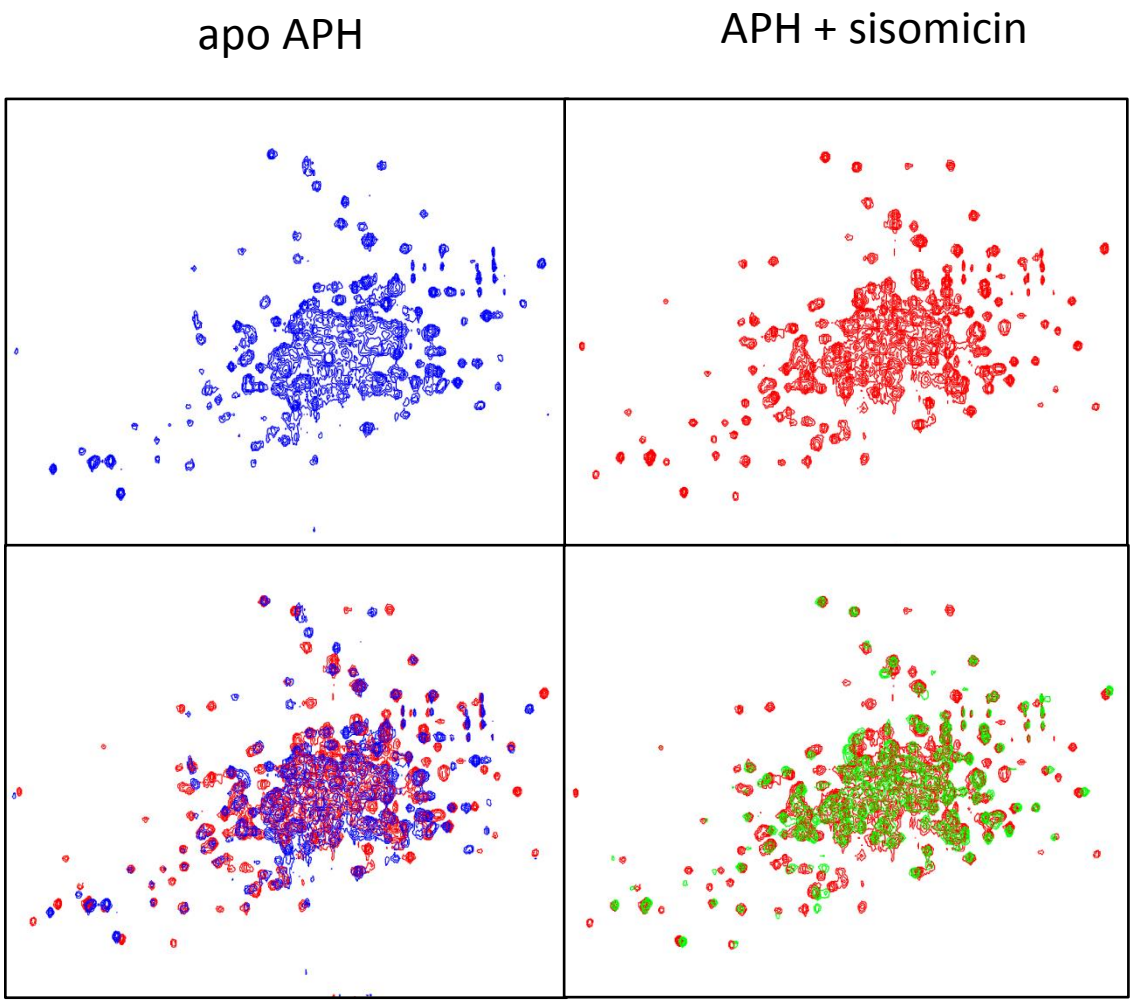


Figure 14: ^{1}H-^{15}N HSQC NMR spectra comparing the peak dispersion of apo APH(blue) top left, and binary APH-sisomicin (red) top right. Overlay images of apo APH(blue) with binary APH-sisomicin (red) on the bottom left. Overlay spectra of binary APH-sisomicin (red) with ternary APH-sisomicin-Mg-AMPPCP (green) on bottom right. All spectra were taken under similar experimental conditions and shown to matching contour levels.

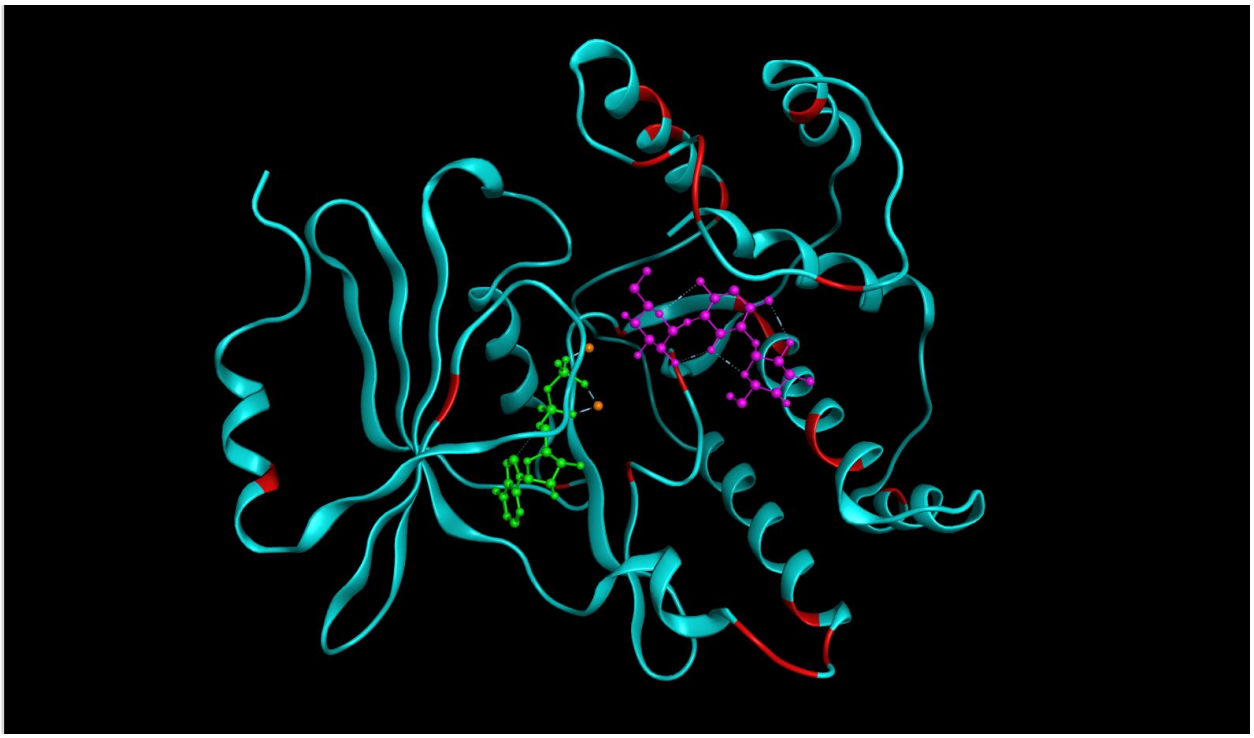


Figure 15: Structure model of APH bound to ADP (green), two Magnesium ions (orange), and kanamycin B (purple). Highlighted in red are the amino acids that showed significant shift in location on the spectra upon APH binding to sisomicin as compared to resonances identified in the binary APH-tobramycin spectra.

Chapter IV: Conclusion and future studies

Exploring the interactions of enzyme APH with its numerous aminoglycoside substrates will provide insight into carbohydrate-protein interactions as well as the discovery of drugs that target these enzymes. By examining the dynamics of APH in the cell, we were able to conclude that the flexible nature of APH that has previously been shown *in vitro* is expected to be true *in vivo*. Therefore the characteristics attributed to APH's flexibility are expected to present *in vivo* as well as *in vitro*. This makes the research previously done with APH and its various substrates even more relevant to clinical application.

It was shown here that in-cell NMR can be used to visualize dynamic protein, APH, in the cell. *In vitro* experiments with BSA showed that APH retains much of its flexibility in crowded environments and the addition of neomycin B causes a gain in global structure. This change in structure was also visualized in NMR spectrum of APH in the lysate. When neomycin B was added to the lysate sample the spectra changed, indicating a change in protein structure. One of the goals for this project was to visualize a change in the structure of APH associated with the binding of an aminoglycoside *in vivo*. However, practical limitations prevented the visualization of structural changes associated with the binding of neomycin to APH in the cell. High concentrations of neomycin caused increased amounts of cell death, which then allowed for cell leakage of proteins from the cell. At lower concentrations of neomycin we were not confident that a significant portion of APH was bound to neomycin in the cell. However, we are confident that neomycin induces structural changes in the cell as this was visualized in both the cell lysate and in the presence of BSA where the protein concentrations were high.

Future directions for in-cell NMR analysis of *in vivo* structural changes of APH includes finding a substrate that is readily imported into the cell but does not cause cell death and the optimization of the induction process or cell line to allow for increased induction time or exposure to aminoglycosides without high amounts of cell death or leakage. In-cell NMR could also be used to compare structured and flexible apo enzymes AAC-IIIb and AAC-IIa in the cell. This comparison would allow look at two relatively similar enzymes, and

determine the differences in spectra of flexible AGMEs and structured AGMEs. This comparison would also provide insight into the natural state of these two enzymes, for example, if AAC-IIIb is typically found bound to CoASH in the cell, then it may be more flexible *in vivo* than it has been shown to be *in vitro*.

There are relatively few published thermodynamic studies with AGMEs; APH is thermodynamically, one of the well characterized AGMEs. This allows for comparisons between the bindings of its various aminoglycoside substrates. The promiscuity of APH is largely attributed to its flexibility which accommodates a large number of aminoglycoside chemical structures. The binding of APH with sisomicin or netilmicin is yet another example of APH's ability to accommodate for structural diversity in its substrates. AAC-IIa is unable to completely accommodate for the additional methyl groups and unsaturated sugar ring of sisomicin. It was shown here that binding of sisomicin to APH, unlike AAC-IIa where part of the enzyme remains unstructured, results in a well-structured complex; similar in conformation to complexes formed with APH and other aminoglycosides. DSC data showed that the melting temperature of binary complex APH-sisomicin was also similar to when APH is bound to other members of the kanamycin group aminoglycosides. The AAC-IIa-sisomicin complex showed a lower melting temperature than complexes of other kanamycins with this enzyme. DSC data also highlighted another difference between these two highly flexible enzymes; APH and its complexes with ligands were all reversible transitions while AAC-IIa denaturation was irreversible. Unlike AAC-IIIb, the order of addition of substrates did not yield ternary APH complexes with different dynamic properties.

Interestingly, the binding of netilmicin to APH highlighted an interesting effect of altered pK_as of titratable groups on the observed binding enthalpy. When binding netilmicin to APH is tested in Tris-HCl, the reaction appeared to be endothermic which is misleading. The reaction is exothermic. However, as the heats of ionization of the buffer increased, its contribution to the observed enthalpy grew to a degree that overwhelmed the actual binding enthalpy. This exemplifies the importance of determining the intrinsic enthalpy of a reaction, especially when there are protonation and deprotonation events occurring. The enthalpies associated with the binding of either sisomicin or netilmicin to APH were much

smaller than APH with other aminoglycosides where the effects of heats of ionization of buffers were smaller.

The formation of the ternary complexes with sisomicin and netilmicin had no effect, or the opposite effect on enthalpy change as compared to the formation of ternary complexes with APH and other aminoglycosides studies to date. An increase in favorable entropy, as seen here, could be attributed to an increase in disorder of water. This may mean that the binding of sisomicin or netilmicin with APH caused a release of more water molecules than previously seen with other aminoglycosides. It is important to note that APH was able to accommodate for these structural differences, unlike AAC-IIa, and we attribute this difference to the flexibility of APH.

In the future, the binary and ternary APH complexes with sisomicin can be further explored with hydrogen-deuterium exchange experiments on NMR to look at the protection of specific amino acids from exchange. HSQC and hydrogen-deuterium exchange NMR experiments could be performed with APH and netilmicin to determine if similar gain in structure is observed with the APH-netilmicin binary complex. DSC experiments could also be performed on APH-netilmicin complexes to compare melting temperatures of the various complexes. This would directly look at the effect of the additional methyl group located on netilmicin's unprimed sugar ring. It was found during this project that AAC-IIa and not AAC-IIIb is able to modify netilmicin, and therefore kinetic and thermodynamic parameters could be examined with AAC-IIa and netilmicin. HSQC NMR experiments with AAC-IIa and netilmicin would provide insight into the effect of the methyl group on the unprimed ring of netilmicin and its effect on the structure of this binary complex in terms of gain in structure or flexibility. Netilmicin is a relatively unexplored aminoglycoside and it would be interesting to examine the binding of this aminoglycoside with various AGMEs.

References

1. Hon, W.C., et al., *Structure of an enzyme required for aminoglycoside antibiotic resistance reveals homology to eukaryotic protein kinases.* Cell, 1997. **89**(6): p. 887-95.
2. Norris, A.L. and E.H. Serpersu, *Ligand promiscuity through the eyes of the aminoglycoside N3 acetyltransferase IIa.* Protein Sci, 2013. **22**(7): p. 916-28.
3. Lahiri, K.D., *Birth of penicillin.* Indian J Vener Dis Dermatol, 1946. **12**(2): p. 17.
4. Clardy, J., M.A. Fischbach, and C.R. Currie, *The natural history of antibiotics.* Curr Biol, 2009. **19**(11): p. R437-41.
5. Waksman, S.A. and H.B. Woodruff, *The Soil as a Source of Microorganisms Antagonistic to Disease-Producing Bacteria.* J Bacteriol, 1940. **40**(4): p. 581-600.
6. Davies, J. and G.D. Wright, *Bacterial resistance to aminoglycoside antibiotics.* Trends Microbiol, 1997. **5**(6): p. 234-40.
7. Vlasits, A.L., et al., *Screen of FDA-approved drug library reveals compounds that protect hair cells from aminoglycosides and cisplatin.* Hear Res, 2012. **294**(1-2): p. 153-65.
8. Drew, R.H. *Aminoglycosides*. Up To Date 2013 9-25-2013 [cited 2013 10/27/2013]; Available from: http://www.uptodate.com/contents/aminoglycosides.
9. Houghton, J.L., et al., *The future of aminoglycosides: the end or renaissance?* Chembiochem, 2010. **11**(7): p. 880-902.
10. Bernacchi, S., et al., *Aminoglycoside binding to the HIV-1 RNA dimerization initiation site: thermodynamics and effect on the kissing-loop to duplex conversion.* Nucleic Acids Res, 2007. **35**(21): p. 7128-39.
11. Schatz, A., E. Bugie, and S.A. Waksman, *Streptomycin, a substance exhibiting antibiotic activity against gram-positive and gram-negative bacteria. 1944.* Clin Orthop Relat Res, 2005(437): p. 3-6.
12. Ramirez, M.S. and M.E. Tolmasky, *Aminoglycoside modifying enzymes.* Drug Resist Updat, 2010. **13**(6): p. 151-71.
13. Rinehart K. L., S.L.S., *Aminocyclitol Antibiotics: An Introduction*, in *Aminocyclitol Antibiotics*, J. Kenneth L. Rinehart, Tetsuo Suami, Editor 1980, American Chemical Society. p. 1-11.
14. Bakker, E.P., *Aminoglycoside and aminocyclitol antibiotics: hygromycin B is an atypical bactericidal compound that exerts effects on cells of Escherichia coli characteristics for bacteriostatic aminocyclitols.* J Gen Microbiol, 1992. **138**(3): p. 563-9.
15. Kotra, L.P., J. Haddad, and S. Mobashery, *Aminoglycosides: perspectives on mechanisms of action and resistance and strategies to counter resistance.* Antimicrob Agents Chemother, 2000. **44**(12): p. 3249-56.
16. Moazed, D. and H.F. Noller, *Interaction of antibiotics with functional sites in 16S ribosomal RNA.* Nature, 1987. **327**(6121): p. 389-94.
17. Woodcock, J., et al., *Interaction of antibiotics with A- and P-site-specific bases in 16S ribosomal RNA.* EMBO J, 1991. **10**(10): p. 3099-103.
18. Vicens, Q. and E. Westhof, *Molecular recognition of aminoglycoside antibiotics by ribosomal RNA and resistance enzymes: an analysis of x-ray crystal structures.* Biopolymers, 2003. **70**(1): p. 42-57.
19. Shaw, K.J., et al., *Molecular genetics of aminoglycoside resistance genes and familial relationships of the aminoglycoside-modifying enzymes.* Microbiol Rev, 1993. **57**(1): p. 138-63.

20. Abraham, E.P. and E. Chain, *An enzyme from bacteria able to destroy penicillin. 1940.* Rev Infect Dis, 1988. **10**(4): p. 677-8.
21. Serpersu, E.H. and A.L. Norris, *Effect of Protein Dynamics and Solvent in Ligand Recognition by Promiscuous Aminoglycoside-Modifying Enzymes.* Advances in Carbohydrate Chemistry and Biochemistry, 2012. **in press**.
22. McKay, G.A., et al., *Recognition of aminoglycoside antibiotics by enterococcal-staphylococcal aminoglycoside 3'-phosphotransferase type IIIa: role of substrate amino groups.* Antimicrob Agents Chemother, 1996. **40**(11): p. 2648-50.
23. Burk, D.L., et al., *Structural analyses of nucleotide binding to an aminoglycoside phosphotransferase.* Biochemistry, 2001. **40**(30): p. 8756-64.
24. Getz, E.B., et al., *A comparison between the sulfhydryl reductants tris(2-carboxyethyl)phosphine and dithiothreitol for use in protein biochemistry.* Anal Biochem, 1999. **273**(1): p. 73-80.
25. McKay, G.A. and G.D. Wright, *Catalytic mechanism of enterococcal kanamycin kinase (APH(3')-IIIa): viscosity, thio, and solvent isotope effects support a Theorell-Chance mechanism.* Biochemistry, 1996. **35**(26): p. 8680-5.
26. McKay, G.A. and G.D. Wright, *Kinetic mechanism of aminoglycoside phosphotransferase type IIIa. Evidence for a Theorell-Chance mechanism.* J Biol Chem, 1995. **270**(42): p. 24686-92.
27. Fong, D.H. and A.M. Berghuis, *Substrate promiscuity of an aminoglycoside antibiotic resistance enzyme via target mimicry.* EMBO J, 2002. **21**(10): p. 2323-31.
28. Serpersu, A.L.N.a.E.H., *NMR Detected Hydrogen-Deuterium Exchange Reveals Differential Dynamics of Antibiotic- and Nucleotide-Bound Aminoglycoside Phosphotransferase 3'-IIIa.* Journal of the American Chemical Society, 2009. **131**(24): p. 8587-94.
29. Serpersu, E.H., et al., *Backbone resonance assignments of a promiscuous aminoglycoside antibiotic resistance enzyme; the aminoglycoside phosphotransferase(3')-IIIa.* Biomol NMR Assign, 2010. **4**(1): p. 9-12.
30. Ozen, C. and E.H. Serpersu, *Thermodynamics of aminoglycoside binding to aminoglycoside-3'-phosphotransferase IIIa studied by isothermal titration calorimetry.* Biochemistry, 2004. **43**(46): p. 14667-75.
31. Jelesarov, I. and H.R. Bosshard, *Isothermal titration calorimetry and differential scanning calorimetry as complementary tools to investigate the energetics of biomolecular recognition.* J Mol Recognit, 1999. **12**(1): p. 3-18.
32. Becker, E.D., *A brief history of nuclear magnetic resonance.* Anal Chem, 1993. **65**(6): p. 295A-302A.
33. Barnes, C.O. and G.J. Pielak, *In-cell protein NMR and protein leakage.* Proteins, 2011. **79**(2): p. 347-51.
34. Serber, Z., et al., *In-cell NMR spectroscopy.* Methods Enzymol, 2005. **394**: p. 17-41.
35. Vanhoof, R., P. Sonck, and E. Hannecart-Pokorni, *The role of lipopolysaccharide anionic binding sites in aminoglycoside uptake in Stenotrophomonas (Xanthomonas) maltophilia.* J Antimicrob Chemother, 1995. **35**(1): p. 167-71.
36. McKay, G.A., P.R. Thompson, and G.D. Wright, *Broad spectrum aminoglycoside phosphotransferase type III from Enterococcus: overexpression, purification, and substrate specificity.* Biochemistry, 1994. **33**(22): p. 6936-44.

37. Molecular Probes, I., *LIVE/DEAD® BacLight™ Bacterial Viability Kits*, I. Molecular Probes, Editor 2004, Invitrogen detection technologies: Eugene, OR.
38. Schneider, C.A., W.S. Rasband, and K.W. Eliceiri, *NIH Image to ImageJ: 25 years of image analysis.* Nat methods, 2012. **9**(7): p. 671-5.
39. Yoshimura, K., A. Toibana, and K. Nakahama, *Human lysozyme: sequencing of a cDNA, and expression and secretion by Saccharomyces cerevisiae.* Biochem Biophys Res Commun, 1988. **150**(2): p. 794-801.
40. Sigma-Alrich, *Lyzsozyme from chicken egg white product information*, Sigma-Aldrich, Editor: St. Louis, MO.
41. Sambrook, J. and D.W. Russell, *Staining SDS-Polyacrylamide Gels with Silver Salts.* CSH Protoc, 2006. **2006**(4).
42. Sambrook, J. and D.W. Russell, *SDS-Polyacrylamide Gel Electrophoresis of Proteins.* CSH Protoc, 2006. **2006**(4).
43. Goddard, T.D. and D.G. Kneller, *SPARKY3*: University of California, San Francisco
44. Delaglio, F., et al., *NMRPipe: a multidimensional spectral processing system based on UNIX pipes.* J Biomol NMR, 1995. **6**(3): p. 277-93.
45. Keswani, N., S. Choudhary, and N. Kishore, *Interaction of weakly bound antibiotics neomycin and lincomycin with bovine and human serum albumin: biophysical approach.* J Biochem, 2010. **148**(1): p. 71-84.
46. Norris, A.L., C. Ozen, and E.H. Serpersu, *Thermodynamics and kinetics of association of antibiotics with the aminoglycoside acetyltransferase (3)-IIIb, a resistance-causing enzyme.* Biochemistry, 2010. **49**(19): p. 4027-35.
47. Hu, X., et al., *Coenzyme A binding to the aminoglycoside acetyltransferase (3)-IIIb increases conformational sampling of antibiotic binding site.* Biochemistry, 2011. **50**(48): p. 10559-65.
48. Sanders, W.E., Jr. and C.C. Sanders, *Sisomicin: a review of eight years' experience.* Rev Infect Dis, 1980. **2**(2): p. 182-95.
49. Wright, E. and E.H. Serpersu, *Molecular determinants of affinity for aminoglycoside binding to the aminoglycoside nucleotidyltransferase(2'')-Ia.* Biochemistry, 2006. **45**(34): p. 10243-50.
50. Norris, A.L. and E.H. Serpersu, *Interactions of coenzyme A with the aminoglycoside acetyltransferase (3)-IIIb and thermodynamics of a ternary system.* Biochemistry, 2010. **49**(19): p. 4036-42.
51. Engel, T., G. Drobny, and P. Reid, *Physical Chemistry for the Life Sciences*, ed. N. Folchetti2008, Upper Saddle River, NJ: Pearson Prentice Hall. 739.
52. Wright, E. and E.H. Serpersu, *Enzyme-substrate interactions with an antibiotic resistance enzyme: aminoglycoside nucleotidyltransferase(2'')-Ia characterized by kinetic and thermodynamic methods.* Biochemistry, 2005. **44**(34): p. 11581-91.
53. Goldberg, R.N., N. Kishore, and R.M. Lennen, *Thermodynamic Quantities for the Ionization Reaction of Buffers.* Journal of Physical Chemistry, 2002. **31**(2): p. 232-370.
54. Wright, E. and E.H. Serpersu, *Effects of Proton Linkage on Thermodynamic Properties of Enzyme-Antibiotic Complexes of the Aminoglycoside Nucleotidyltransferase (2'')-Ia.* J Thermodyn Catal, 2011. **2**(1): p. 6.
55. Hegde, S.S., et al., *Thermodynamics of aminoglycoside and acyl-coenzyme A binding to the Salmonella enterica AAC(6')-Iy aminoglycoside N-acetyltransferase.* Biochemistry, 2002. **41**(23): p. 7519-27.

56. Ozen, C., J.M. Malek, and E.H. Serpersu, *Dissection of aminoglycoside-enzyme interactions: a calorimetric and NMR study of neomycin B binding to the aminoglycoside phosphotransferase(3')-IIIa.* J Am Chem Soc, 2006. **128**(47): p. 15248-54.
57. Dam, T.K. and C.F. Brewer, *Thermodynamic studies of lectin-carbohydrate interactions by isothermal titration calorimetry.* Chem Rev, 2002. **102**(2): p. 387-429.
58. Jing, X., et al., *Thermodynamic characterization of a thermostable antibiotic resistance enzyme, the aminoglycoside nucleotidyltransferase (4').* Biochemistry, 2012. **51**(45): p. 9147-55.
59. Magalhaes, M.L. and J.S. Blanchard, *The kinetic mechanism of AAC3-IV aminoglycoside acetyltransferase from Escherichia coli.* Biochemistry, 2005. **44**(49): p. 16275-83.
60. Boehr, D.D., et al., *Analysis of the pi-pi stacking interactions between the aminoglycoside antibiotic kinase APH(3')-IIIa and its nucleotide ligands.* Chem Biol, 2002. **9**(11): p. 1209-17.

Vita

To the great joy of her parents, Stephen and Dawn Rosendall, Katelyn Dawn Rosendall was born on October 7, 1988. She is the younger sister to Ryan Rosendall and the older sister to Danae Rosendall. She grew up in Hudsonville, Michigan attending Hudsonville public schools until her graduation from Hudsonville High School in May 2007. In August 2007 Katelyn moved south to attend Lee University. While there, she majored in Biology and gained experience in both laboratory and field sciences. During the summer of 2010, Katelyn traveled abroad to Australia to study the various ecosystems present there. She completed her bachelors of Science degree from Lee University in May 2011. She then moved north to spend the summer of 2011 working as the environmental education director at Camp Henry in Newaygo, Michigan. After a challenging and fun summer spent working at a summer camp, she traveled back to Tennessee in August 2011 to attend graduate school at The University of Tennessee in the department of biochemistry, cellular and molecular biology. She completed work on her thesis in December 2013 and received her M.S. in biochemistry, cellular and molecular biology in May 2014. She is planning to gain additional teaching experience before pursuing her Doctorate of Philosophy in Science Education from Western Michigan University.